REVIEW ARTICLE

Research Progress on Propagation of Vortex Beams in Atmospheric Turbulence

Xiwen Li[1], **Jingyuan Liang**[1] **and Xizheng Ke**[1,2,*]

[1] School of Automation and Information Engineering, Xi'an University of Technology, Xi'an 710048, China
[2] Shaanxi Provincial Key Laboratory of Intelligent Collaborative Network for Civil-Military Integration, Xi'an 710048, China

Abstract

Vortex beams carrying orbital angular momentum enable a new multiplexing dimension for optical wireless communications. However, atmospheric turbulence induces beam broadening, intensity scintillation, beam wander, angle-of-arrival fluctuations, and OAM crosstalk, degrading propagation performance. This review summarizes the fundamental theories of vortex beams and atmospheric turbulence, analyzes turbulence-induced effects, and surveys domestic and international research progress, introduces representative research achievements of the team from Xi'an University of Technology, and finally prospects the future development directions of this field.

Keywords: orbital angular momentum, atmospheric turbulence, vortex beam, propagation characteristics, turbulence effect.

Submitted: 21 April 2026
Accepted: 19 May 2026
Published: 02 July 2026

Vol. 1, **No.** 1, 2026.
10.62762/OWC.2026.800222

***Corresponding author:**
✉ Xizheng Ke
xzke@xaut.edu.cn

1 Introduction

The development of communication technologies has always been closely associated with advances in science and technology and the growing demand for information interaction in human society. With the popularization of high-bandwidth applications such as high-definition video and cloud computing, the requirements for high speed, security, and large capacity in information transmission continue to rise. Optical communication, featuring abundant bandwidth resources, high transmission rates, and strong immunity to electromagnetic interference, has become a core technology supporting modern high-capacity communication networks [1]. Optical communication is divided into two major branches: wired optical communication and optical wireless communications [2]. Among them, optical wireless communications require no physical transmission medium and possess the characteristics of flexible deployment, no need for spectrum licensing, and rapid networking. These advantages are further enhanced when combined with advanced modulation schemes such as OFDM to improve spectral efficiency and robustness [3]. However, the propagation process of optical wireless communications is susceptible to atmospheric turbulence. Random fluctuations in the atmospheric refractive index give rise to problems including optical intensity scintillation, wavefront

Citation
Li, X., Liang, J., & Ke, X. (2026). Research Progress on Propagation of Vortex Beams in Atmospheric Turbulence. *Optical Wireless Communication*, 1(1), 4–29.

distortion, and spot wander, which degrade the stability of signal transmission. Meanwhile, the Gaussian beam adopted in conventional optical wireless communications carries information in a single dimension, making it difficult to meet the exponentially growing demands for transmission capacity in next-generation communication systems [4]. These two issues have become key factors restricting the high-performance development of optical wireless communications.

The discovery of vortex beams provides an effective solution to the above problems [5]. Their unique helical wavefront structure enables them to carry orbital angular momentum (OAM). On the basis of conventional modulation dimensions such as amplitude, phase, and frequency, as well as multiplexing techniques including wavelength division, time division, and code division, vortex beams add a new information dimension of orbital angular momentum to optical wireless communications. Vortex beams with different topological charges can realize orbital angular momentum mode multiplexing, allowing multiple signals to be transmitted in parallel and independently within the same channel, which significantly improves communication capacity and spectral efficiency. Accordingly, vortex optical communication is regarded as an important development direction for next-generation high-performance optical wireless communication systems [5]. To fully exploit the technical advantages of vortex optical communication, it is essential to characterize the propagation properties of vortex beams in real atmospheric environments. Their wavefront and orbital angular momentum features lead to more complex propagation and evolution laws than those of Gaussian beams. Investigating their propagation characteristics and analyzing the influence mechanism of atmospheric turbulence constitutes a critical step in promoting vortex optical communication from theoretical research to practical applications. Relevant studies can not only improve the theoretical system of vortex beam propagation in complex environments but also provide guidance for the application of vortex optical communication systems, possessing important theoretical and practical values.

At present, scholars have carried out extensive research on the propagation characteristics of vortex beams in atmospheric turbulence. Nevertheless, existing studies still lack universal analytical models capable of quantifying different turbulence effects. Taking the propagation characteristics of vortex beams under atmospheric turbulence as the core research focus, this paper systematically reviews the domestic and international research progress in this field, presents the research achievements of the team from Xi'an University of Technology in vortex beam-related areas, summarizes the existing problems in current research, and finally prospects future research directions and development trends in this field. It is expected to provide references for the follow-up research on vortex beam propagation characteristics and the optimal design of vortex optical communication systems.

2 Theory of Vortex Beams and Propagation in Atmospheric Turbulence

2.1 Vortex Beams

Vortex beams represent a class of optical fields with distinctive phase or polarization characteristics. Since they carry orbital angular momentum (OAM), they are also referred to as OAM beams. According to their spatial structural features, vortex beams are mainly categorized into two types. One is the phase vortex beam, as illustrated in Figure 1, whose wavefront exhibits a continuous helical phase distribution. The other is the vector vortex beam, which not only carries OAM but also possesses a specific polarization state distribution in the cross-section of the optical field. This paper focuses on phase vortex beams, which are simply referred to as "vortex beams" hereinafter [5].

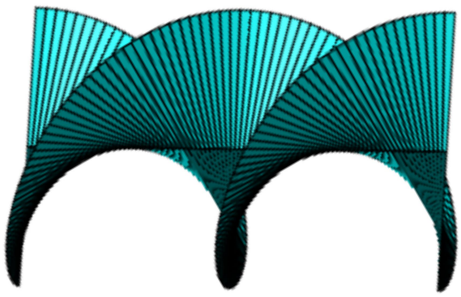

Figure 1. Vortex optical wavefront.

The complex amplitude expression of a vortex beam can be written as:

$$E(\rho,\theta,z) = E_0(\rho,z)\exp(i\phi(\rho,z))\exp(il\theta) \quad (1)$$

where $E(\rho,\theta,z)$ is referred to as the l-th order vortex beam; (ρ,θ,z) denotes the polar coordinates of the vortex beam's cross-section; z represents the propagation distance of the vortex beam in space; $E_0(\rho,z)$ is the amplitude of the beam; $\phi(\rho,z)$ is the

initial phase of the beam; and $\exp(il\theta)$ is the helical phase factor with order l. When $l = 0$, the vortex beam loses its helical phase characteristics and the optical field distribution reduces to a conventional Gaussian beam.

The key to the applicability of vortex beams in optical wireless communications lies in the infinite-valued property and orthogonality of their orbital angular momentum (OAM). Specifically, the infinite-valued property refers to the fact that OAM values can theoretically cover all integers; the orthogonality, meanwhile, is manifested in the mutual orthogonality of vortex beams carrying different OAM values in their spatial modes. For any two vortex beams, their optical field distributions can be expressed as:

$$E_1(\rho, z) = A_1(\rho, z) \exp(il_1\theta) \tag{2}$$

where $E_1(\rho, z)$ is the complex amplitude of the first vortex beam at propagation distance z and radial coordinate ρ; $A_1(\rho, z)$ is the amplitude distribution of the first vortex beam; l_1 is the topological charge of the first vortex beam; θ is the azimuthal coordinate in the cylindrical coordinate system.

$$E_2(\rho, z) = A_2(\rho, \theta) \exp(il_2\theta) \tag{3}$$

where $E_2(\rho, z)$ is the complex amplitude of the second vortex beam at propagation distance z and radial coordinate ρ; $A_2(\rho, \theta)$ is the amplitude distribution of the second vortex beam; l_2 is the topological charge of the second vortex beam; θ is the azimuthal coordinate in the cylindrical coordinate system.

The azimuthal integration of the inner product of Equations (2) and (3) yields:

$$\int_0^{2\pi} E_1 E_2^* \, d\theta = A_1 A_2^* \, \delta(l_2 - l_1) = \begin{cases} A_1 A_2^*, & l_1 = l_2 \\ 0, & l_1 \neq l_2 \end{cases} \tag{4}$$

where E_1 and E_2^* denote the complex amplitude of the first vortex beam and the complex conjugate of the second vortex beam, respectively; θ is the azimuthal coordinate integrated over the full circle $[0, 2\pi]$; A_1 and A_2^* are the amplitude of the first vortex beam and the complex conjugate of the amplitude of the second vortex beam, respectively; $\delta(\cdot)$ is the Dirac delta function; l_1 and l_2 are the topological charges of the two vortex beams.

2.2 Introduction to Atmospheric Turbulence

As illustrated in Figure 2, both turbulence and laminar flow are forms of fluid motion. The distinction between them is as follows: the velocity and flow direction of fluid in laminar flow are steady, whereas fluid in turbulent flow exhibits vortical motion with random movement directions and irregular vortex scales. Turbulence essentially satisfies the Navier–Stokes (NS) equations [6]. However, it is not only spatiotemporally chaotic and highly fluctuating but also characterized by multi-scale coupling and dissipation. Meanwhile, turbulent motion varies randomly around its statistical mean. These features make it nearly impossible to derive analytical solutions for turbulent motion from a theoretical perspective, and various engineering approaches have been developed to mitigate the resulting propagation degradation [7].

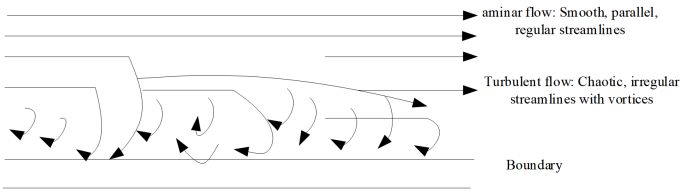

Figure 2. Schematic diagram of laminar flow and turbulent flow.

Atmospheric turbulence is a typical random inhomogeneous medium and a special form of fluid motion. Characterized by pronounced randomness and inhomogeneity, it commonly occurs in the atmospheric boundary layer, the interior of convective clouds, and the upper tropospheric westerly jet stream regions, where wind shear and thermal gradients significantly affect the laser beam propagation in satellite–ground optical links [8]. Wind shear induced by near-surface airflow drag, differential surface heating due to solar radiation, and thermal convection driven by surface thermal radiation cause random variations in atmospheric temperature and velocity fields. These random temperature fluctuations, in turn, lead to stochastic changes in wind speed, atmospheric density, and atmospheric pressure, ultimately giving rise to atmospheric turbulence. Its existence significantly enhances the exchange of momentum, heat, and water vapor in the atmosphere, and also causes random fluctuations in the atmospheric refractive index—whose characteristics are closely related to atmospheric temperature, humidity, and wind shear instability [9]. Vortices generated by atmospheric turbulence are continuously formed and annihilated as they move rapidly with the wind. The

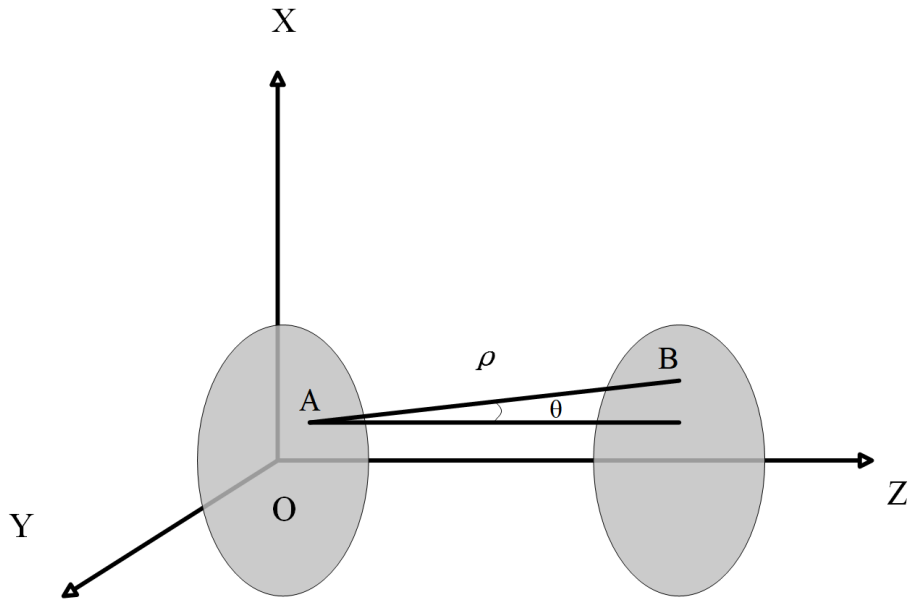

Figure 3. Schematic diagram of Huygens-Fresnel principle.

cyclic process of vortex formation and dissipation, combined with the superposition of their motions, eventually forms random turbulent motion, which defines atmospheric turbulence [9].

2.3 Optical Wave Propagation Theory

2.3.1 Generalized Huygens–Fresnel Integral Formula

As an extended form of the classical Huygens–Fresnel principle, the generalized Huygens–Fresnel integral has been widely adopted to analytically characterize the propagation of optical fields through inhomogeneous media, including atmospheric turbulence [10]. As illustrated in Figure 3, this principle states that every point on a wavefront can be regarded as a new secondary wave source radiating spherical secondary waves; the wavefront at a subsequent moment is formed by the envelope of all these secondary waves, and the optical vibration at any point in space arises from the coherent superposition of these secondary waves. Its mathematical expression is given as [11].

$$E(\rho, z) = -\frac{i}{2\lambda} \iint E_0(x, y, 0) \frac{\exp(ik\rho)(1 + \cos\theta)}{\rho} \, dx \, dy \tag{5}$$

where $E(\rho, z)$ denotes the complex amplitude at the observation field; $E_0(x, y, 0)$ represents the complex amplitude at the light source; ρ is the distance between the source point and the field point; and θ is the angle between the normal n at the source point and the distance ρ.

When the applicable conditions for the Fresnel approximation are satisfied, i.e., when the distance z between the diffraction plane and the observation plane is much greater than the linear dimensions of the diffraction aperture and the observation region [12].

$$\rho \approx z, \quad \cos\theta \approx 1, \quad z \gg |x_2 - x_1|, \ |y_2 - y_1| \tag{6}$$

the Huygens–Fresnel integral formula can be further expressed as [13].

$$E(\rho, z) = -\frac{ik}{2\pi z} \exp(ikz) \iint E_0(\rho, 0) \exp\left[\frac{ik}{2z}|\rho - \rho_0|^2\right] d^2\rho_0 \tag{7}$$

The expression for the optical field of a light wave after propagating a distance z in a turbulent medium is [14].

$$E(\rho, z) = -\frac{ik}{2\pi z} \exp(ikz) \iint E_0(\rho, 0) \exp\left[\frac{ik}{2z}|\rho - \rho_0|^2 + \Psi(\rho, \rho_0)\right] d^2\rho_0 \tag{8}$$

where $\Psi(\rho, \rho_0)$ denotes the random complex phase perturbation of the optical field during propagation in the turbulent medium.

2.3.2 Born Approximation

The Born approximation, which assumes light wave propagation along the positive z-axis, treats the optical field perturbations as additional contributions to the unperturbed optical field, i.e., the total optical field can be expressed as a linear superposition of the unperturbed optical field and perturbation terms. The perturbation terms can be written as

$$E(\mathbf{R}) = E_0(\mathbf{R}) + E_1(\mathbf{R}) + E_2(\mathbf{R}) + \cdots \tag{9}$$

where $E_0(\mathbf{R})$ is the unperturbed optical field in the absence of turbulence, and the remaining

terms correspond to the first-order perturbation term, second-order perturbation term, and higher-order perturbation terms arising from random inhomogeneities, respectively.

Given $E_0(\mathbf{R})$, $E_1(\mathbf{R})$ can be expressed as

$$E_1(\mathbf{R}) = \iiint \mathbf{G}(\mathbf{S},\mathbf{R}) \left[2k^2 n_1(\mathbf{S}) E_{\text{free}}(\mathbf{S})\right] d\mathbf{S} \quad (10)$$

where $\mathbf{G}(\mathbf{S},\mathbf{R}) = \mathbf{G}(\mathbf{R},\mathbf{S})$ is the free-space Green's function, given by

$$G(\mathbf{S},\mathbf{R}) = \frac{1}{4\pi|\mathbf{R}-\mathbf{S}|}\exp(ik|\mathbf{R}-\mathbf{S}|) \quad (11)$$

Due to the small scattering angle of the optical wave, we introduce cylindrical coordinate representations for $\mathbf{R}$ and $\mathbf{S}$

$$\mathbf{R} = (\rho, z), \quad \mathbf{S} = (s, L) \quad (12)$$

Under the paraxial approximation, the Green's function is written as

$$\begin{aligned} &G(\mathbf{S},\mathbf{R}) \equiv G(\mathbf{S},\rho;z,L) \\ &= \frac{1}{4\pi(z-L)}\exp\left[ik(z-L) + \frac{ik}{2(z-L)}|\mathbf{S}-\rho|^2\right] \end{aligned} \quad (13)$$

Thus, the first-order perturbation term within the Born approximation can be expressed as

$$\begin{aligned} \Phi_1(\rho,z) = \frac{k^2}{2\pi}\int_0^z dL \iint_0^\infty ds \exp\left[ik(z-L) + \frac{ik|\mathbf{S}-\rho|^2}{2(z-L)}\right] \\ \times E_{\text{free}}(\mathbf{S},L)\frac{n_1(\mathbf{S},L)}{z-L} \end{aligned} \quad (14)$$

In solving the second-order perturbation under the Born approximation, we obtain the following result using the Green's function method

$$\begin{aligned} \Phi_2(\rho,z) = \frac{k^2}{2\pi}\int_0^z dL \iint_0^\infty ds \exp\left[ik(z-L) + \frac{ik|\mathbf{S}-\rho|^2}{2(z-L)}\right] \\ \times E_1(\mathbf{S},L)\frac{n_1(\mathbf{S},L)}{z-L} \end{aligned} \quad (15)$$

Similarly, the i-th order perturbation term can be expressed as

$$\begin{aligned} \Phi_i(\rho,z) = \frac{k^2}{2\pi}\int_0^z dL \iint_0^\infty ds \exp\left[ik(z-L) + \frac{ik|\mathbf{S}-\rho|^2}{2(z-L)}\right] \\ \times E_{i-1}(\mathbf{S},L)\frac{n_1(\mathbf{S},L)}{z-L}, \quad i = 1,2,3\cdots \end{aligned} \quad (16)$$

While the expressions for higher-order perturbation terms are straightforward to derive, they have not been extensively studied to date. Consequently, the applicability of the Born approximation to light wave propagation is severely limited, primarily due to its insufficient accuracy in scenarios involving multiple scattering, strong scattering, and inelastic scattering in inhomogeneous media. Furthermore, the method only performs a first-order series expansion of the wave equation under high-frequency fluctuations, failing to account for higher-order term analyses and resulting in a marked reduction in its effectiveness.

2.3.3 *Rytov Perturbation Theory*

The main distinction between the Born approximation and the Rytov perturbation method lies in that the Born approximation is based on the addition of perturbation terms to the unperturbed term, whereas the Rytov perturbation method is based on the multiplication of perturbation terms with the unperturbed term. According to the Rytov method, the optical field after propagating through turbulence can be written as:

$$U(\rho) = U_0(\rho,z)\exp[\psi(\rho,z)] \quad (17)$$

where $\psi(\rho,z)$ denotes the complex phase perturbation caused by turbulence, which takes the form

$$\psi(\rho,z) = \psi_1(\rho,z) + \psi_2(\rho,z) + \psi_3(\rho,z) + \cdots \quad (18)$$

where $\psi_i(\rho,z)$ $(i = 1,2,3)$ represent the first-order, second-order, and third-order complex phase perturbations induced by turbulence, respectively.

By establishing a relationship between the Rytov perturbation terms and the previously calculated Born perturbation terms, we introduce the normalized Born perturbation

$$\Phi_j(\rho,z) = \frac{E_j(\rho,z)}{E_0(\rho,z)} \quad j = 1,2,3\cdots \quad (19)$$

For computational convenience, we set the first-order Rytov perturbation equal to the Born perturbation

$$\begin{aligned} E_0(\rho,z)\exp[\psi_1(\rho,z)] &= E_0(\rho,z) + E_1(\rho,z) \\ &= E_0(\rho,z)[1+\Phi_1(\rho,z)] \end{aligned} \quad (20)$$

Dividing both sides of the above equation by $E_0(\rho,z)$ and taking the logarithm yields the first-order Rytov perturbation as:

$$\psi_1(\rho,z) = \ln[1+\Phi_1(\rho,z)] \approx \Phi_1(\rho,z) \quad \Phi_1(\rho,z) \ll 1 \quad (21)$$

where

$$\begin{aligned}\Phi_1(\rho,z) &= \frac{E_1(\rho,z)}{E_0(\rho,z)} \\ &= \frac{k^2}{2\pi}\int_0^z dL\int_0^\infty \exp\left[ik(z-L)+\frac{ik|s-\rho|^2}{2(z-L)}\right] \\ &\times \frac{E_0(s,L)}{E_0(\rho,L)}\frac{n_1(s,L)}{z-L}\,ds\end{aligned} \tag{22}$$

where $E_0(\rho,z)$ denotes the optical field in the receiving plane; $E_0(s,L)$ denotes the optical field on an arbitrary plane along the propagation path.

By equating the second-order perturbation terms of the Born and Rytov approximations, we obtain:

$$\begin{aligned}&E_0(\rho,z)\exp[\psi_1(\rho,z)+\psi_2(\rho,z)] \\ &\quad = E_0(\rho,z)+E_1(\rho,z)+E_2(\rho,z) \\ &\quad = E_0(\rho,z)[1+\Phi_1(\rho,z)+\Phi_2(\rho,z)]\end{aligned} \tag{23}$$

Dividing both sides of the above equation by $E_0(\rho,z)$ and taking the logarithm yields the second-order Rytov perturbation as:

$$\begin{aligned}&\psi_1(\rho,z)+\psi_2(\rho,z) \\ &= \ln[1+\Phi_1(\rho,z)+\Phi_2(\rho,z)] \\ &\approx \Phi_1(\rho,z)+\Phi_2(\rho,z)-\frac{1}{2}\Phi_1^2(\rho,z) \\ &\quad |\Phi_1(\rho,z)|\ll 1,\ |\Phi_2(\rho,z)|\ll 1\end{aligned} \tag{24}$$

On the right-hand side of Equation (24), the second-order terms of the Maclaurin series are retained. Since $\psi_1(\rho,z)=\Phi_1(\rho,z)$, the second-order Rytov perturbation term can be obtained:

$$\psi_2(\rho,z)=\Phi_2(\rho,z)-\frac{1}{2}\Phi_1^2(\rho,z) \tag{25}$$

$$\begin{aligned}\Phi_2(\rho,z) &= \frac{E_2(\rho,z)}{E_0(\rho,z)} \\ &= \frac{k^2}{2\pi}\int_0^z dL\int_0^\infty ds\,\exp\left[ik(z-L)+\frac{ik|s-\rho|^2}{2(z-L)}\right] \\ &\times \frac{\Phi_1(s,z)E_0(s,z)\eta_1(s,z)}{E_0(\rho,z)(z-L)}\end{aligned} \tag{26}$$

In the research on the propagation of optical wave fields in weak turbulent fluctuation regions, most studies only use first-order perturbation, which is sufficient to calculate the log-amplitude variance, phase variance, intensity and phase correlation functions, and wave structure functions. However, to obtain the statistical moments of the optical field from Rytov theory, both the first-order perturbation term ψ_1 and the second-order perturbation term ψ_2 must be considered simultaneously.

2.4 Turbulence Effects

2.4.1 Intensity Scintillation

As illustrated in Figure 4, intensity scintillation refers to the phenomenon in which a beam undergoes scattering and diffraction by multiple independent turbulent eddies when propagating through the turbulent atmosphere, resulting in random fluctuations of the light intensity in the received spot. These fluctuations are directly related to the strength of turbulence, manifesting as the light intensity varying with time and randomly fluctuating around its mean value [11]. The intensity scintillation variance is a statistical quantity that describes the phase and intensity fluctuations of an optical wave caused by turbulence during propagation in a turbulent medium [12]. Under weak fluctuation conditions, the scintillation index is defined as the normalized variance of intensity fluctuations [13].

$$\sigma_I^2=\exp\left(4\chi^2\right)-1\equiv\sigma_R^2,\quad \sigma_R^2\ll 1 \tag{27}$$

where χ^2 denotes the log-amplitude fluctuation variance; σ_R^2 denotes the Rytov variance; σ_I^2 denotes the scintillation index.

The scintillation index can be expressed as:

$$\sigma_I^2(z)=\frac{\left\langle I^2(z)\right\rangle-\left\langle I(z)\right\rangle^2}{\left\langle I(z)\right\rangle^2} \tag{28}$$

where $I(z)$ is the light intensity; $\langle\cdot\rangle$ denotes the ensemble average.

The log-amplitude fluctuation variance of a plane wave under the Kolmogorov turbulence power spectrum can be expressed as [13]:

$$\chi^2_{\text{plane}}=0.307C_n^2k^{7/6}L^{11/6} \tag{29}$$

where k is the wavenumber, related to the propagation wavelength λ; C_n^2 denotes the atmospheric refractive index structure parameter; and L represents the propagation distance.

The log-amplitude fluctuation variance of a spherical wave can be expressed as:

$$\chi^2_{\text{sphere}}=0.124C_n^2k^{7/6}L^{11/6} \tag{30}$$

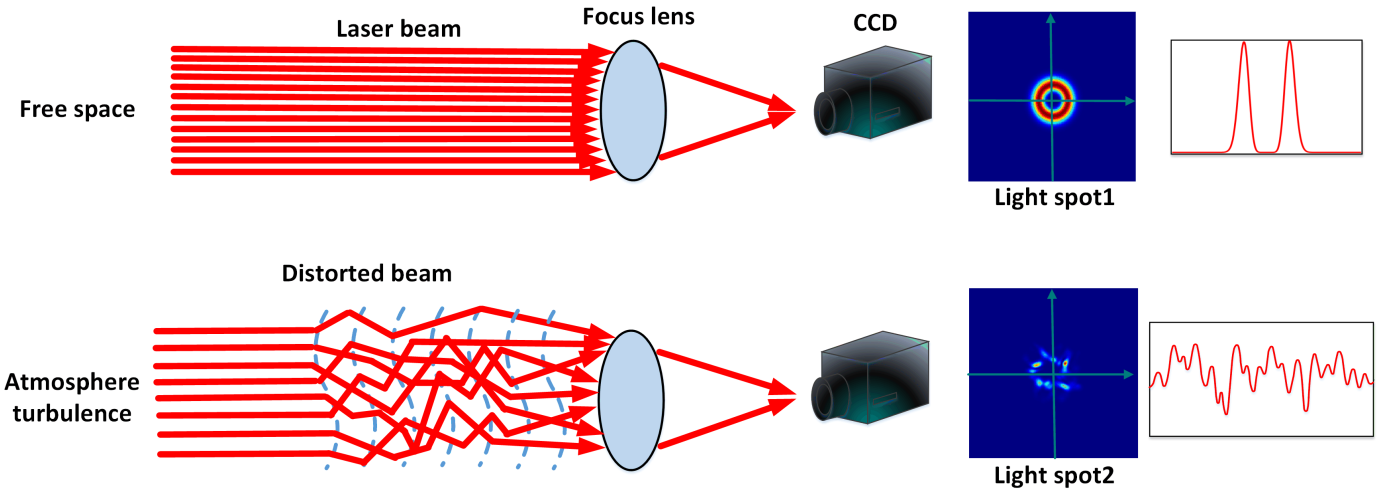

Figure 4. Schematic Diagram of Light Intensity scintillation [14].

The log-amplitude fluctuation variance of a Gaussian beam can be expressed as:

$$\chi^2 = \pi^2 \left(0.033 C_n^2\right) \Gamma(-5/6) k^{7/6} L^{11/6} \left\{ \frac{\alpha L}{1+(\alpha L)^2} \right\}^{5/6} \times \left\{ \frac{3}{8} \cdot {}_1F_1 \left[-\frac{5}{6}, 1; \frac{2\rho^2}{\omega_0^2 \left[1+(\alpha L)^2\right]} \right] - g(\alpha L) \right\} \tag{31}$$

where ρ denotes the radial distance; Γ denotes the Gamma function; λ denotes the propagation wavelength, with $k = 2\pi/\lambda$; ω_0 denotes the beam waist radius; ${}_1F_1(a, c; z)$ denotes the confluent hypergeometric function; and $\alpha = \lambda/\pi\omega_0^2$:

$$g(\alpha L) = \mathrm{Re}\left(\frac{6}{11}\right) \left(\frac{1+i\alpha L}{i\alpha L}\right)^{5/6} \cdot {}_2F_1\left(-\frac{5}{6}, 1; \frac{17}{6}; i\alpha L\right) \tag{32}$$

where ${}_2F_1(a, c; z)$ is the Gaussian hypergeometric function.

2.4.2 Beam Broadening

As shown in Figure 5, under ideal propagation conditions, the laser beam is focused onto the surface of the photodetector by a coupling lens, completing photoelectric conversion to generate an electrical signal, with almost no loss of beam energy during this ideal transmission process. When propagating through atmospheric turbulence, the beam broadens due to fluctuations in the atmospheric refractive index, and the energy in the beam cross-section decreases, resulting in a portion of the beam failing to reach the photodetector surface through the coupling lens [12].

After being perturbed by atmospheric turbulence, the beam width of a Gaussian beam is expressed as [16]:

$$W_{\mathrm{LTG}} = W\sqrt{1 + 1.636 \cdot C_n^2 \cdot k^{1/3} \cdot z^{8/3} \cdot W^{-5/3}} \tag{33}$$

where $W = \omega_0\sqrt{1+(z/z_R)^2}$ denotes the Gaussian beam radius in free space; $z_R = \pi\omega_0^2/\lambda$ denotes the Rayleigh range; and C_n^2 denotes the atmospheric refractive index structure parameter, which characterizes the strength of turbulence; ω_0 is the initial beam waist radius in free space at the transmitter plane; z is the propagation distance; $k = 2\pi/\lambda$ is the wavenumber.

2.4.3 Beam Wander

As illustrated in Figure 6, atmospheric turbulence disturbs the beam during propagation, causing the phenomenon of beam wander. This wander induces random displacements of the beam in the direction perpendicular to the optical axis, resulting in deviations from the receiving plane. The optical axis of the transmitted beam and the boresight axis of the receiving antenna no longer coincide and subtend an angle, which shifts the focal point of the beam converged by the optical antenna. Consequently, the shifted focal point cannot be incident on the receiving surface of the photodetector. The beam power received by the photodetector therefore decreases significantly, which adversely affects signal detection [12].

Beam wander is typically quantified by the coordinate variation of the beam spot centroid, whose expression is given by [17]:

$$\rho_c = \frac{\iint I(\rho, z)\rho \, d\rho \, d\theta}{\iint I(\rho, z) \, d\rho \, d\theta} \tag{34}$$

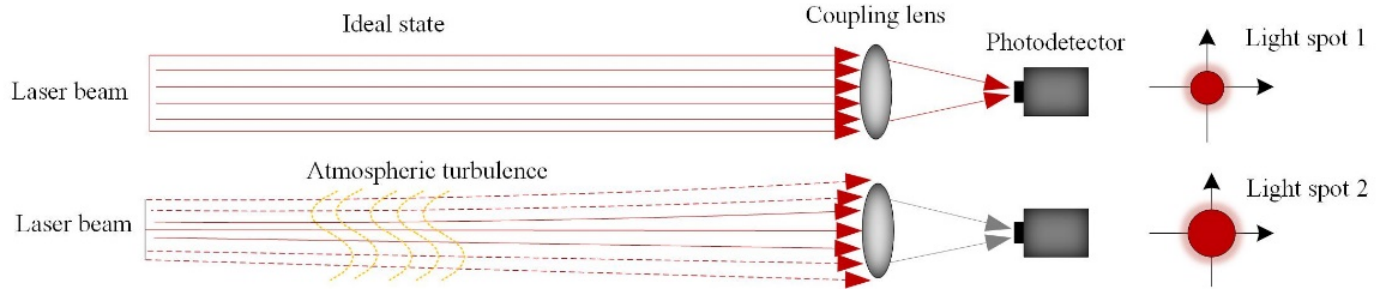

Figure 5. Schematic diagram of beam broadening [15].

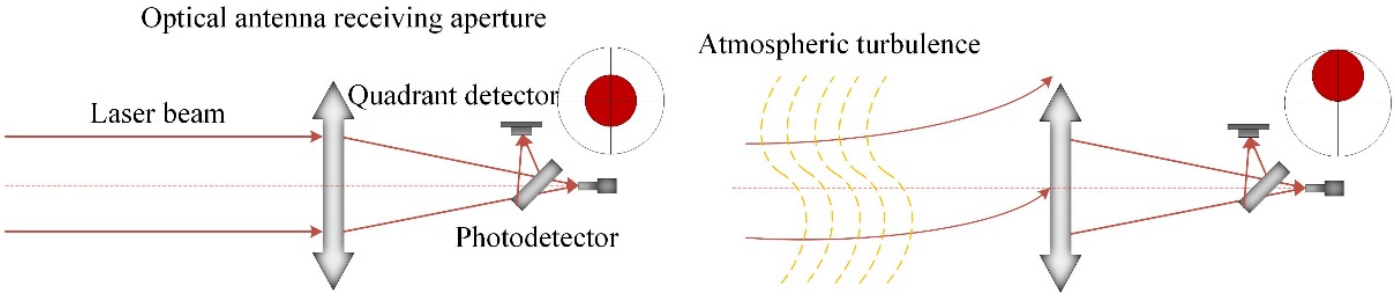

Figure 6. Schematic diagram of beam wander [15].

where $I(\rho, z)$ denotes the optical field intensity at the receiver; ρ is the radial coordinate from the beam axis; z is the propagation distance; θ is the azimuthal angle around the beam axis, ranging from 0 to 2π.

The centroid coordinates are:

$$x_c = \frac{\iint I(x,y)x\,dx\,dy}{\iint I(x,y)\,dx\,dy} \tag{35}$$

$$y_c = \frac{\iint I(x,y)y\,dx\,dy}{\iint I(x,y)\,dx\,dy} \tag{36}$$

where x and y are Cartesian coordinates.

The degree of beam wander is characterized by the variance of the beam spot centroid wander, expressed as:

$$\rho_c^2 = \frac{\iiint I(\rho_1)I(\rho_2)\rho_1\rho_2\,d\rho_1\,d\rho_2}{\left(\iiint I(\rho)\,d\rho\right)^2} \tag{37}$$

For a Gaussian beam propagating through atmospheric turbulence, combined with the power-law power spectrum model, the corresponding beam wander variance is given by:

$$\langle r_c^2\rangle = 2.42C_n^2 z^3 \omega_0^{-1/3}\left[1-\left(\frac{\kappa_0^2\omega_0^2}{1+\kappa_0^2\omega_0^2}\right)^{1/6}\right], \tag{38}$$

$$\kappa_0 = \frac{1}{L_0}$$

where κ_0 is the spatial wavenumber scalar corresponding to the outer scale L_0.

2.4.4 *Angle-of-Arrival Fluctuations*

When a beam propagates through atmospheric turbulence, the beam divergence angle observed at the receiving plane is defined as the angle of arrival. During propagation, the angle of arrival undergoes random fluctuations due to turbulence perturbations, resulting in continuous variations in the angle of arrival of the beam wavefront. This phenomenon is referred to as the angle-of-arrival fluctuation effect [12]. The local angle of arrival is illustrated in Figure 7.

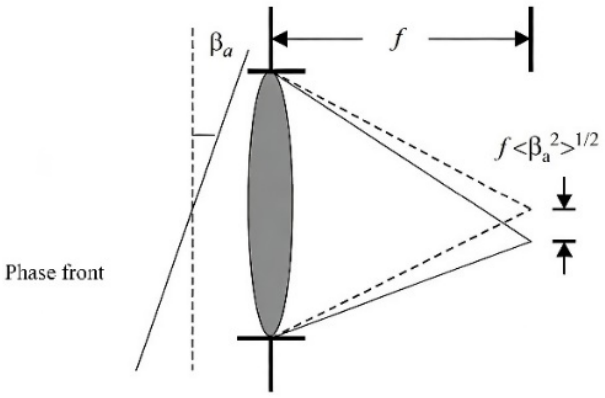

Figure 7. Schematic diagram of the local angle of arrival.

Under the Kolmogorov spectrum condition, the angle-of-arrival fluctuation variance of a plane wave after propagating through atmospheric turbulence is

given by [16]:

$$\left\langle \beta_a^2 \right\rangle = \begin{cases} 1.64 C_n^2 L l_0^{1/3} \\ \quad \times \left[1 - 0.72 \left(k_0 l_0 \right)^{1/3} \right], & 2W_G \ll l_0 \\ 2.91 C_n^2 L \left(2W_G \right)^{-1/3} \\ \quad \times \left[1 - 0.81 \left(2k_0 W_G \right)^{1/3} \right], & 2W_G \gg l_0 \end{cases} \tag{39}$$

where $2W_G$ is the diameter of the receiving antenna aperture; l_0 is the inner scale of turbulence, representing the smallest eddy size, note that this l_0 is a turbulence parameter and is different from the topological charge l used elsewhere for vortex beam order.

From Eq. (39), it can be seen that the angle-of-arrival variance of a plane wave increases with the increase of turbulence strength and propagation distance.

For a spherical wave propagating through atmospheric turbulence, its angle-of-arrival fluctuation variance is defined as:

$$\left\langle \beta_a^2 \right\rangle = 2.91 C_n^2 L \left(2W_G \right)^{-1/3}, \quad 2W_G \gg l_0 \tag{40}$$

From Eq. (40), it can be seen that the angle-of-arrival fluctuation variance of a spherical wave increases with the increase of turbulence strength and propagation distance.

2.4.5 Orbital Angular Momentum Crosstalk

The turbulence effects induced by atmospheric turbulence on the propagation of vortex beams—including intensity scintillation, beam wander, and beam broadening—do not exist independently of one another. These effects interact with each other during propagation and all originate from the wavefront distortion of vortex beams caused by turbulence perturbations, serving as direct manifestations of wavefront distortion. The combined action of these effects destroys the helical phase structure that carries information in vortex beams, which manifests as OAM mode crosstalk in the modal domain. Unlike the universality of other turbulence effects, OAM mode crosstalk represents a core problem unique to vortex beams.

When an OAM beam propagates through atmospheric turbulence, its vortex phase becomes distorted, causing the OAM spectral distribution to no longer concentrate on the initial OAM mode carried by the original optical field. Instead, energy diffuses from the initial OAM mode to adjacent OAM modes. This phenomenon is referred to as OAM mode crosstalk [18]. At present, most studies on OAM mode crosstalk are carried out based on the phase screen method, combined with the spiral spectrum expansion method. The spiral spectrum is defined as:

$$P = C_l / \sum_{q=-\infty}^{\infty} C_q \tag{41}$$

where C_q is the energy of each order of spiral harmonics, and C_l is the energy carried by different spiral harmonic indices l. The spiral spectrum can be used to analyze the OAM mode crosstalk of vortex beams after propagation through atmospheric turbulence.

Taking a single OAM beam as an example, after propagating through atmospheric turbulence, new adjacent modes are generated at the receiver end due to the inhomogeneous distribution of the refractive index in the turbulent medium. As a result, the beam modes can no longer be clearly distinguished and separated. Figure 8 shows a schematic diagram of OAM beam mode crosstalk.

3 Research Progress on Atmospheric Turbulence Propagation of Vortex Beams

3.1 Discovery and Generation of Vortex Beams

In physics, the propagation of waves is conventionally studied by solving the regular solutions of the wave equation. Nye and Berry [19] pointed out that singularities can occasionally arise in the solutions of the wave equation. Such singularities are characterized by physical quantities at certain points in space becoming infinitely large (or infinitely small) or undergoing abrupt changes; these special points are known as singular points. The existence of singular points often gives rise to a series of singular phenomena.

In 1974, Nye and Berry [19] observed a fixed rule during his investigation of the evolution of cotidal lines and tidal peaks: multiple cotidal lines converge at a single point and rotate around it, after which the tidal peak vanishes and the tidal level at this point is zero. This point represents a phase singularity in tidal waves. The vortical flow surrounding such a singular point is referred to as a vortex, which exists widely in nature—examples include water whirlpools, ocean circulations, tornadoes in the atmosphere, and spiral galaxies in the Milky Way.

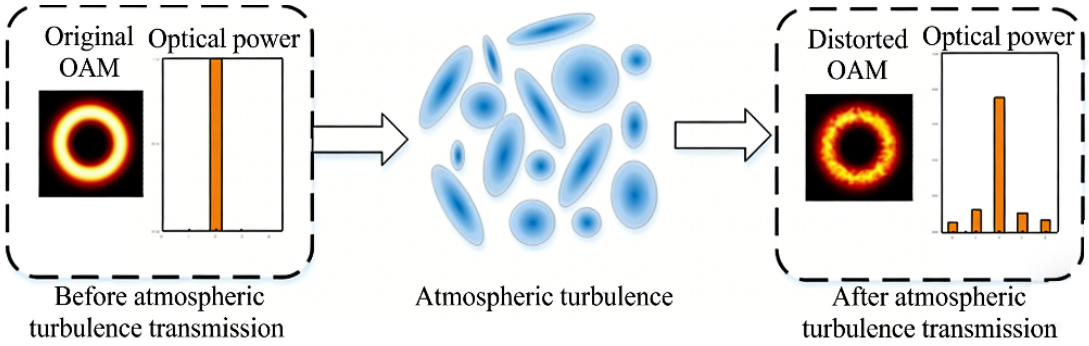

Figure 8. Schematic diagram of OAM beam mode crosstalk [18].

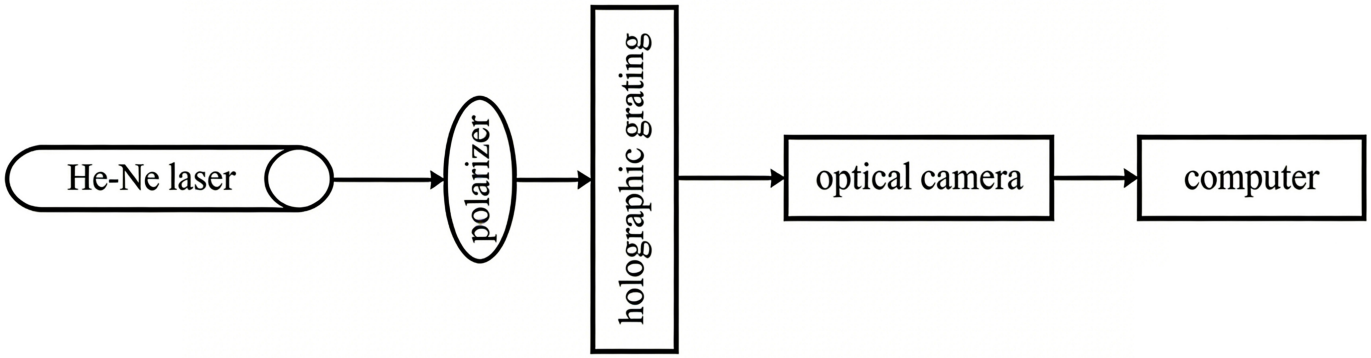

Figure 9. Schematic diagram of computer-generated hologram for vortex beam generation.

Vortical phenomena are not only present in macroscopic natural scenarios but also in optical-related fields. Vortex phenomena in optical fields have been extensively studied in the context of partially coherent beams, where the phase singularity structure and its evolution under various propagation conditions have been systematically analyzed [20]. Subsequently, Braunbek, Wolf, Boivin, and others discovered and verified the existence of optical vortices in interference fields and energy-flow fields, respectively [21].

In 1989, inspired by hydrodynamic vortices, Coullet et al. [22] found vortex solutions to the Maxwell–Bloch equations in optical fields and explicitly put forward the concept of an optical vortex. Then, in 1992, Allen et al. [23] discovered that each photon in a vortex beam carrying helical wavefront dislocations possesses an orbital angular momentum (OAM) of $\hbar l$ (where l denotes the topological charge of the beam). This discovery revealed a new connection between macroscopic optics and quantum effects and provided researchers with a renewed understanding of optical vortices.

Since the 1980s, vortex beams have attracted extensive attention from researchers due to their excellent performance in particle manipulation, super-resolution imaging and optical measurement, and a variety of methods for generating vortex beams have been developed.

In 1994, Barnett and Allen [24] investigated the relationship between axisymmetric beams and orbital angular momentum (OAM) under non-paraxial approximation conditions. Theoretical derivations confirmed that any beam containing the term $e^{il\theta}$ carries OAM. This conclusion laid a theoretical foundation for the introduction and study of various OAM-carrying beams beyond Laguerre–Gaussian (LG) beams. In the same year, based on Allen's OAM theory, Beijersbergen et al. [25] experimentally generated LG vortex beams using a spiral phase plate (SPP), establishing the core principle of generating vortex beams via direct phase modulation.

In 1995, He et al. [26] successfully produced Laguerre–Gaussian beams using holographic techniques and realized the manipulation of microscopic particles with such beams. Figure 9 illustrates the principle of generating vortex beams via computer-generated holography (CGH), which

can be summarized in four key steps: first, define the optical field of the target vortex beam; then perform high-precision sampling of the target optical field; next, select an appropriate encoding scheme to encode the sampled data and generate a computer-generated hologram; finally, complete experimental observation and verification.

Based on experimental studies of Laguerre–Gaussian beams, researchers soon began to expand the physical scope of vortex beams. In 1987, Durnin [27] proposed the theoretical model of non-diffracting Bessel beams. In 2002, Volke-Sepúlveda et al. [28] experimentally observed that high-order Bessel beams also carry orbital angular momentum, and systematically analyzed the OAM state characteristics of Bessel beams with helical and radial polarizations, promoting the development of Bessel vortex beams from theoretical verification to practical research. Regarding the generation of non-diffracting Bessel beams, in 2021, Khonina et al. [29] designed a lens-like axicon structure using a spherical lens with spherical aberration, and carried out simulations and experiments combined with geometrical optics ray tracing, successfully generating non-diffracting Bessel beams.

Since the 21st century, the research focus on vortex beam generation has shifted from "whether vortex beams can be generated" to "how to generate them in a simpler, more stable, and application-adaptable manner." Multiple technical routes based on traditional optical components have gradually matured, forming the mainstream solution system still widely used today. The spiral phase plate (SPP) method has become the most widely adopted vortex beam generation scheme of this stage, owing to its straightforward principle, simple optical path, and high beam purity. In 2008, Xie and Zhao [30] successfully generated vortex beams using a spiral phase plate. The SPP method produces vortex beams by modulating the phase distribution of light waves. Its core principle is to introduce a spiral phase factor via the SPP during beam propagation, endowing the light wave with orbital angular momentum. Figure 10 shows a spiral phase plate with thickness s, refractive index n, and azimuthal angle θ. When a Gaussian beam is incident on the SPP, a vortex beam is generated.

The rapid development of micro-nano fabrication technology has brought paradigm-shifting innovation to the manipulation of vortex beam optical fields. Research at this stage broke away from the

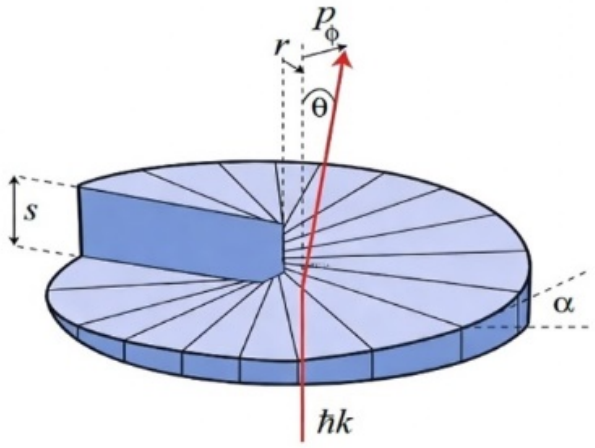

Figure 10. Spiral phase plate.

conventional logic of phase modulation relying on optical path differences in traditional optical components, ushering in a new development phase of on-chip integration. In 2011, Yu et al. [31] published the landmark work in the field of metasurfaces in Science, proposing the generalized Snell's laws of reflection and refraction. Using nanoscale V-shaped antenna metasurface structures, the work realized precise localized control over the phase, amplitude, and polarization of light waves at the subwavelength scale, and successfully generated vortex beams with metasurfaces for the first time.This work completely eliminated the size constraints of traditional bulk optical components, providing a new technical path for the planarization, integration, and miniaturization of vortex beam generation devices. It also opened up a new research direction for manipulating vortex optical fields in metaphotonics.

To meet the core demand for flexible switching of vortex beams in laboratory settings, the programmable dynamic modulation scheme based on the Spatial Light Modulator (SLM) shown in Figure 11 has gradually become a universal standard in laboratories.

In 2016, Forbes et al. [32] addressed the shortcomings of low mode purity and insufficient modulation accuracy in traditional schemes by optimizing the encoding and modulation methods of digital holograms. By rewriting digital holograms in real time to dynamically control the phase modulation process of the SLM, OAM beams with different topological charges and mode types could be generated on demand, realizing high-speed, high-precision, and fully dynamic programmable modulation of vortex optical fields, and further improving the practicality

Figure 11. Actual spatial light modulator.

of this scheme.

With the maturity of mainstream technical solutions, the research focus of vortex beam generation has shifted toward deviceization, customization, and performance optimization for practical application scenarios. Aiming at the core requirements of different scenarios such as integrated large-capacity optical communication and micro-nano particle manipulation, researchers have carried out targeted optimization on key indicators including device integration and modulation accuracy, leading to the emergence of a series of technical schemes.

To satisfy the application demand of vortex beams in fiber-optic communication, in 2017, Wang et al. [33] studied the orbital angular momentum multiplexing technology of vortex beams and successfully realized vortex beam generation using few-mode fibers.

For the on-chip application demand of vortex beams in integrated optoelectronic systems, in 2017, Du and Wang [34] designed a compact and easily integrable silicon-based integrated optical vortex lattice generator. The device consists of three parallel silicon waveguides and etched tilted gratings, which can regulate the output direction through gratings and finally generate vortex beams with topological charges of $l = \pm 1$.

To solve the problems of high processing difficulty and limited topological charge modulation accuracy of traditional bulk spiral phase plates, in 2013, Zelenchuk and Fusco [35] designed a planar spiral phase plate (SPP) for vortex beam generation, which can precisely control the topological charge of vortex beams, and the beam generation accuracy is gradually improved with the increase of phase orders.

To meet the core demand of mode dimension expansion for large-capacity orbital angular momentum multiplexing communication systems, in 2023, Xu et al. [36] successfully obtained fractional-order dual vortex beams by coaxial superposition of two vortex beams with different fractional-order topological charges. The propagation direction and field pattern distribution of dual vortex beams can be flexibly controlled by adjusting the fractional values of the inner and outer ring topological charges, providing a novel structured optical field for multi-dimensional manipulation of microparticles.

Building on the idea of generating complex vortex optical fields via superposition, Zhao et al. [37] experimentally verified in 2025 the generation scheme of double-ring vortex beams by superposing beams with identical or opposite topological charges.

To overcome the inherent defect of traditional Laguerre–Gaussian vortex beams that the spot radius expands with increasing topological charge, limiting particle manipulation accuracy, in 2024, Liu et al. [38] realized the generation of perfect vortex beams with different topological charges. Based on geometric phase modulation technology, the team designed a single-metal-layer metasurface, enabling the generated vortex beams to maintain a constant radial intensity distribution under different topological charges and exhibit excellent structural stability.

In summary, over the past three decades, the research and development of vortex beams have always centered on the core direction of enhancing controllability. With the continuous advancement of optical technology, their generation methods have gradually evolved from traditional optical components to integrated optical devices. A variety of implementation schemes have now been formed, including spiral phase plates, spatial light modulators, metasurface structures, and others [39, 40], demonstrating overall development characteristics of diversification, integration, and high efficiency.

3.2 Propagation of Vortex Beams

The atmosphere is an unavoidable natural propagation medium for free-space laser transmission, and the external-field propagation of vortex beams inevitably takes the atmosphere as its carrier. As a typical randomly inhomogeneous medium, the atmosphere

causes a series of propagation degradation effects in propagating vortex beams, such as wavefront distortion, intensity scintillation, and beam wander, which in turn severely restrict the overall operational performance of optoelectronic systems.

Long before the advent of lasers, Tatarski et.al [11] had investigated the characteristics of light wave propagation in turbulent media, including beam broadening, intensity scintillation, and coherence evolution. However, early studies on light propagation in random media remained relatively fragmented. With the emergence and continuous improvement of laser technology, laser-based systems such as lidar, space communication equipment, and laser-guided weapons have developed rapidly. Most of these devices operate in random media such as atmospheric turbulence and oceanic turbulence, which has promoted research on the propagation characteristics of beams in random media. During this period, the academic community gradually established a variety of analytical methods for light propagation in random media, including the Rytov perturbation method, geometrical optics method, parabolic equation method, generalized Huygens–Fresnel principle, and statistical moment equations of the optical field. Among them, the geometrical optics method and Rytov approximation can effectively solve beam propagation problems under weak fluctuation conditions; the statistical moment equation of the optical field derived based on the Markov approximation can yield approximate solutions for strong fluctuation scenarios, while research on moderate-intensity fluctuations still mainly relies on numerical simulations [42].

In the last century, research objects of beam propagation were mainly focused on spherical waves, plane waves, and Gaussian beams. Since the beginning of the 21st century, researchers worldwide have carried out extensive studies on the propagation characteristics of novel structured light beams in atmospheric turbulence, including partially coherent beams with complex spatial coherence structures [43], laying the groundwork for subsequent investigations into vortex beams. In addition, many scholars have proposed various spectral methods for simulating atmospheric turbulence perturbations, among which the turbulence statistical moment theoretical model and the extended Huygens–Fresnel principle are among the most widely adopted analytical frameworks, with the validity and applicability of these approaches under various turbulence regimes having been critically discussed [42]. The former is mainly used to explore phase perturbation, wavefront distortion, and intensity fluctuation in turbulent media; the latter is mostly applied to analyze the degradation of beam propagation quality in turbulence and to conduct measurements of turbulence distribution.

In recent years, with the continuous expansion of the application scope of vortex beams in complex scenarios such as free-space propagation, atmospheric turbulence, and oceanic turbulence, research on their propagation characteristics under atmospheric turbulence has increasingly become a core hotspot in the field of optical field manipulation.

As a typical atmospheric turbulence effect, intensity scintillation and the associated light intensity evolution law constitute key research contents in this field. In 2009, Eyyuboğlu et al. [44] analyzed the propagation characteristics of modified Bessel-Gaussian vortex beams in weak turbulent atmosphere by using the extended Huygens–Fresnel principle and Rytov approximation theory, and derived the analytical expression of the scintillation index during turbulent propagation. The results show that, under the same source size parameters, this beam can effectively suppress the scintillation effect caused by atmospheric turbulence. Meanwhile, an increase in the inner scale of turbulence enhances the scintillation effect, whereas the influence of the outer scale is relatively weak. In 2011, Berman et al. [45] explored the propagation characteristics of combined Gaussian vortex beams in atmospheric channels based on the Kolmogorov turbulence power spectrum model combined with the Rytov approximation theory, and deduced the analytical expression of the scintillation index during turbulent transmission. Studies show that this beam can effectively suppress the scintillation effect during propagation. In 2015, Xu et al. [46] combined the Kolmogorov turbulence spectrum with the generalized Huygens–Fresnel principle to thoroughly investigate the propagation characteristics of partially coherent Laguerre–Gaussian beams in atmospheric channels, and derived analytical expressions for their intensity distribution and effective beam width. The research indicates that, compared with fully coherent Laguerre–Gaussian beams, the intensity of partially coherent beams is less affected by atmospheric turbulence perturbations. In 2010, Li et al. [47] combined the Kolmogorov turbulence spectrum with the generalized Huygens–Fresnel principle to study the propagation characteristics of partially coherent off-axis vortex beams, and derived the analytical expression of light intensity

distribution during propagation. The results reveal a significant positive correlation between beam broadening and coherence length, beam waist width, propagation distance, and turbulence strength. In 2016, Liu et al. [48] explored the propagation properties of partially coherent four-petal Gaussian vortex beams in turbulent atmosphere based on Fresnel diffraction theory. By analyzing the beam propagation characteristics under different parameter conditions, the regular variation of the distortion dispersion degree of the two beams with parameters was clarified. In 2021, Hricha et al. [49] derived the analytical expressions for the cross-spectral density function and average light intensity of vortex Hermite-cosine-hyperbolic-Gaussian beams after propagation in turbulent media, based on the Kolmogorov turbulence power spectrum, extended Huygens–Fresnel diffraction integral, and Rytov approximation theory. The influence of turbulence intensity on the intensity distribution with varying beam parameters was analyzed in depth. In 2025, Chen et al. [50] investigated the propagation characteristics of double Laguerre–Gaussian beams in oceanic turbulent media, focusing on the influence of different turbulence parameters on the scintillation index. The results show that the scintillation index increases correspondingly when the turbulent energy dissipation rate decreases gradually, while the propagation distance and temperature variance dissipation rate increase synchronously, leading to a reduced system bit error rate.

The above studies demonstrate that various beams carrying vortex phases exhibit a certain resistance to intensity scintillation caused by atmospheric turbulence compared with non-vortex beams.

Beam broadening occurs during the propagation of beams through atmospheric turbulence, resulting in degraded reception performance of communication systems. This effect also constitutes an important research direction for the propagation characteristics of vortex beams.

In this direction, researchers have explored the broadening characteristics of various types of vortex beams under atmospheric turbulence by deriving analytical expressions. In 2025, Odžak [51] systematically investigated the propagation of standard and elegant Laguerre–Gaussian vortex beams through a gradient-index medium via theoretical derivation, analyzing the beam broadening characteristics and intensity evolution under varying medium parameters, providing complementary insight into vortex beam broadening in structured inhomogeneous media beyond atmospheric turbulence. In 2011, Zhong et al. [52] conducted an in-depth study on the propagation characteristics of partially coherent Laguerre–Gaussian (LG) beams in atmospheric turbulence based on the extended Huygens–Fresnel principle combined with the second-order moment analysis method of the Wigner distribution function (WDF). The angular width variation and quantitative characteristics of the beam propagation factor after transmission were investigated. In 2012, Lukin et al. [53] carried out a thorough study on the beam broadening characteristics of LG beams in random media based on the Kolmogorov turbulence power spectrum model and numerical modeling. Analytical expressions for the beam width of propagating LG beams in turbulent environments were derived, and the specific influences of topological charge and turbulence strength on the beam broadening effect were analyzed. Results show that beams with larger topological charges exhibit higher broadening rates in turbulent media, and the broadening rate accelerates significantly with increasing turbulence strength. In 2006, Zhou [54] studied the angular spectrum diffraction theory of vortex beams, focusing on the vector far-field propagation characteristics of Laguerre–Gaussian beams. Research indicates that after propagation in turbulent environments, the intensity distribution of such beams shows divergent features, and the degree of intensity divergence becomes more pronounced as the topological charge increases. In 2020, Luo and Han [55] systematically derived analytical expressions for the intensity distribution of arbitrary-order vortex beams and their arrays propagating in turbulent media based on the generalized Huygens–Fresnel principle and Rytov approximation theory, and numerically investigated the broadening characteristics and evolution laws of the beams. By analyzing the mean-square beam width variation under different beam and turbulence parameters, results show that vortex beam arrays are less disturbed by turbulence than single-mode vortex beams, and radial vortex beam arrays gradually evolve into a Gaussian-like beam distribution during long-distance propagation. In 2022, Lazrek et al. [56] systematically simulated the beam broadening characteristics and average intensity evolution of vortex cosine-hyperbolic-Gaussian beams in oceanic turbulence based on the extended Huygens–Fresnel diffraction theory, and explored the influence mechanisms of key parameters such as

mean-square temperature and temperature-salinity fluctuation dissipation rate on the propagation characteristics. In 2023, Pan et al. [57] investigated the propagation characteristics of rotationally symmetric power-exponent-phase vortex beams in oceanic turbulence. Based on the extended Fresnel diffraction theory combined with an oceanic turbulence model, the influence of propagation distance on the intensity distribution of vortex beams was analyzed. Results show that the light intensity of vortex beams gradually weakens with increasing propagation distance, while the spot spreading effect is significantly enhanced. This study provides important theoretical support for the application of vortex beams in underwater optical communication.

The above studies show that vortex beams exhibit broadening characteristics after turbulent propagation, which becomes more severe with increasing topological charge, while the relative beam width decreases with increasing topological charge.

Researchers have also investigated the singularity drift, beam wander, orbital angular momentum (OAM) crosstalk, and diffusion effects of partial vortex beams during propagation in atmospheric turbulence.

In 2005, Flossmann et al. [58] thoroughly explored the far-field diffraction intensity distribution of off-axis Laguerre–Gaussian (LG) beams based on Fresnel diffraction theory, and for the first time clarified the regulatory effect of the topological charge sign on the movement direction of beam singularities, providing a new theoretical perspective for optimizing the propagation characteristics of vortex beams. In 2024, Padgett [59] reviewed the quantum fundamentals of orbital angular momentum at the single-photon level, discussing how the OAM state of individual photons is affected during propagation through turbulent environments and providing theoretical insight into the angular momentum characteristics of photons under turbulence-induced perturbations. In 2019, Zeng et al. [60] explored the evolution characteristics of OAM in Laguerre–Gaussian beams under weak atmospheric turbulence based on the Rytov perturbation theory, and derived the integral analytical formula of the OAM spectrum after atmospheric turbulence propagation. Studies show that both increased turbulence strength and longer propagation distance lead to a significant aggravation of OAM spectrum diffusion, showing a clear positive correlation with the degree of spectrum diffusion. In 2014, Yao et al. [61] theoretically investigated the propagation of electromagnetic stochastic beams in anisotropic atmospheric turbulence, analyzing the effects of turbulence anisotropy parameters on the beam spreading and coherence characteristics during transmission. The study reveals that turbulence anisotropy significantly modifies the spatial coherence degradation of the beam compared with isotropic turbulence models. In 2023, Wei et al. [62] derived the analytical expression of the spiral spectrum for focused perfect vortex beams propagating in atmospheric turbulence based on spiral spectrum analysis theory, and explored the evolution of OAM characteristics after turbulent propagation. Studies show that the degree of crosstalk between OAM modes is significantly positively correlated with increased propagation distance, enhanced turbulence strength, and enlarged topological charge.

Since the turbulence characteristics in early studies were all processed under the assumption of homogeneity and isotropy, this idealized turbulence serves as the foundation of the Kolmogorov statistical theory of turbulence. As early as the 1970s, experiments had revealed that atmospheric turbulence does not always obey the Kolmogorov distribution. By the 1990s, a growing body of experimental data had further validated this observation. Researchers therefore revised the Kolmogorov turbulence theory and introduced the concept of non-Kolmogorov turbulence.

To describe the complex real atmospheric environment more accurately, some scholars have adopted the non-Kolmogorov spectrum, anisotropic turbulence model, and slant propagation model to investigate the propagation characteristics of vortex beams. The mode power spectrum of Laguerre–Gaussian beams propagating in Kolmogorov turbulence has also been analyzed using analytical methods, revealing how turbulence-induced modal coupling redistributes energy across OAM modes [41]. In 2013, Jiang [63] studied the propagation characteristics of Laguerre–Gaussian (LG) beams based on the non-Kolmogorov turbulence spectrum, derived the analytical expression of the spiral spectrum, and analyzed the dynamic evolution of the OAM spectrum distribution after the beams propagated through non-Kolmogorov turbulence. Results show that both increased turbulence strength and longer propagation distance significantly enhance the distortion of the OAM spectrum, showing a clear positive correlation with the degree of influence. In 2011, Cerjan, A. and Cerjan, C. [64]

theoretically analyzed the orbital angular momentum of Laguerre–Gaussian beams beyond the paraxial approximation, deriving the weight of each spiral harmonic component in the total beam energy and investigating how non-paraxial propagation conditions affect the OAM content. The study indicates that the OAM of the beam is affected by the spatial inhomogeneity of the atmosphere. In 2020, Lv et al. [65] derived the analytical expression for the orbital angular momentum spectrum of partially coherent vortex beams during slant atmospheric turbulence propagation based on the Rytov approximation theory, examined the evolution of OAM mode purity, and explored the influence mechanisms of propagation distance, turbulence strength, and zenith angle on the diffusion characteristics of the spiral spectrum. Results show that the OAM mode purity decreases significantly and the spiral spectrum diffusion intensifies with increasing turbulence strength, longer propagation distance, and larger zenith angle. This study provides a key theoretical basis for the precise manipulation of beam OAM characteristics in slant propagation scenarios. In 2016, Cheng [66] established a propagation model for Bessel–Gaussian (BG) beams based on the Rytov theory under the framework of the generalized anisotropic von Karman turbulence spectrum, and explored the effects of turbulence anisotropy and source parameters on the detection probability of OAM modes. The study shows that the anisotropic property of turbulence can improve the transmission performance of OAM modes. In 2023, Wang et al. [67] developed a theoretical model that separates the effect of anisotropy from other turbulence parameters to calculate the spiral spectrum of twisted Laguerre-Gaussian Schell-model beams after propagation through anisotropic turbulence in horizontal links, and investigated the influence of anisotropy on the probability density of the OAM spectrum and its mode crosstalk. In 2021, Guo et al. [68] derived the analytical expression for OAM crosstalk of partially coherent Bessel–Gaussian localized waves after propagation through anisotropic turbulence using the Rytov theory, and analyzed the OAM crosstalk characteristics of such beams in weak-to-strong anisotropic atmospheric turbulence channels. Results show that, compared with conventional BG beams, the OAM modes carried by these beams exhibit better propagation stability and anti-interference capability in turbulent environments, with significantly improved transmission quality. In 2021, Murakami et al. [69] derived the analytical expression of the spiral spectrum and the formula of intensity distribution for Gaussian vortex beams after slant atmospheric propagation. The study shows that the degree of spiral spectrum diffusion increases with longer propagation distance, and is significantly aggravated under the conditions of stronger near-ground turbulence and smaller inner turbulence scale. This achievement breaks through the framework limitation of the classical Kolmogorov theory by constructing a physical model that is more consistent with the actual atmospheric environment.

Since theoretical methods such as the Rytov perturbation method are only applicable to weak turbulence regions, numerical simulations are still widely used in domestic and international research to analyze the propagation characteristics of vortex beams under moderate-intensity atmospheric turbulence [70]. In 2011, Liu and Pu [71] used the random phase screen technique to observe the propagation characteristics of elliptical vortex beams in turbulent media and analyzed the evolution of scintillation along the propagation path. Results show that, compared with conventional beams, the scintillation index of vortex beams at the axial position can be effectively suppressed, demonstrating excellent anti-turbulence interference capability. In 2014, Rodenburg et al. [72] employed the phase screen technique to construct a simulated atmospheric turbulence environment and systematically carried out experimental research on the propagation characteristics of OAM beams in turbulent media. Results reveal significant mode crosstalk during OAM beam propagation, with a clear positive correlation between crosstalk intensity and turbulence strength. In 2014, Banakh and Falits [73] focused on the broadening characteristics of LG beams in atmospheric turbulence and numerically analyzed the intensity distribution after propagation. The study indicates that, in turbulent media, the turbulent broadening of LG beams relative to diffractive broadening is independent of the beam mode and mainly depends on the diffraction region at the transmitting aperture. In terms of absolute broadening, the turbulent broadening amplitude of LG beams increases with increasing topological charge. In 2017, Porfirev et al. [74] used the multi-phase screen technique to simulate the propagation characteristics of low-order Laguerre–Gaussian beams in aerosol optical media and explored the evolution of beam intensity and mode structure along the propagation path. Results show a significant positive correlation between beam broadening, increased turbulence strength,

and extended propagation distance. In the same year, Fu [75] used the multi-phase screen method to simulate the propagation of Bessel–Gaussian (BG) beams and LG beams in atmospheric turbulence, and discussed the influences of turbulence strength, propagation distance, and beam type on OAM mode crosstalk and mode purity. Results show that the helical phase distribution is deformed by turbulence perturbations, and the deformation becomes more severe with stronger turbulence. In the same year, Filimonov et al. [76] numerically studied the dynamic variation characteristics of orbital angular momentum of LG beams propagating in atmospheric turbulence, and investigated the influence of beam-receiver axial alignment deviation on the mean and variance of OAM fluctuations. In the same year, Eyyuboğlu [77] used the random phase screen method to thoroughly explore the evolution of scintillation characteristics of vortex beams in strong turbulence. Results show that the scintillation effect continuously decreases as the topological charge increases, but the reduction rate gradually slows down with a further rise in topological charge. In 2009, Wang and Zheng [78] analyzed the propagation characteristics of optical vortices formed by coherent laser beam arrays in atmospheric turbulence. Experiments show that the stability of vortex beams is generally weaker than that of Gaussian beams in short-distance propagation, but exhibits a distinct advantage in long-distance transmission. This property is speculated to be closely related to their self-reconstruction ability after passing through obstacles. In 2018, Ke Xizheng [18] applied the multi-phase screen technique to simulate atmospheric turbulence and explored the crosstalk characteristics of OAM multiplexed beams during turbulent propagation via spiral spectrum analysis. Results indicate that increased turbulence strength significantly aggravates crosstalk between OAM modes, showing a positive correlation with turbulence intensity. In 2025, Li [79] used the multi-phase screen technique to simulate the propagation characteristics of vector vortex beams in atmospheric turbulence, and found that they exhibit lower scintillation index and beam wander in long-distance transmission, verifying their remarkable advantages in suppressing turbulence perturbations. In 2025, Su [80] used the multi-phase screen technique to systematically investigate the evolution of intensity distribution and variation of the axial scintillation factor of dual elliptical vortex beams propagating in atmospheric turbulence. Results show that the axial scintillation factor of this beam is lower than that of single elliptical vortex beams, but gradually increases with increasing turbulence strength. This work confirms that vortex beams combining elliptical structure and polarization properties possess stronger anti-turbulence interference capability.

In recent years, numerous significant advances have been achieved in the research on propagation characteristics of novel vortex beams in atmospheric turbulence. Double-ring perfect vortex beams exhibit stable beam radius and excellent anti-wander performance during propagation in atmospheric turbulence [81]. Robust measurement of orbital angular momentum can be realized for partially coherent vortex beams under the condition of amplitude and phase perturbations [82]. Vortex beams propagating in anisotropic atmospheric turbulence present significant spiral spectrum broadening and OAM mode crosstalk, whose degree is closely correlated with propagation distance, turbulence anisotropy, and topological charge [83]. A physics-driven untrained neural network provides an effective solution for vortex beam wavefront compensation in adaptive optics-aided underwater wireless optical communication systems [84]. Vector anomalous vortex beams show distinct propagation behaviors of orbital angular momentum in maritime atmospheric turbulence environments [85]. Ring Airy vortex beams and ring Pearcey vortex beams display different evolution regularities during propagation in turbulent atmosphere [86]. Autofocusing Mathieu vortex beams present unique propagation dynamics when propagating through atmospheric turbulence [87]. The intensity distribution and degree of coherence of vortex beams show regular evolution characteristics in atmospheric turbulence [88]. The above latest research results enrich the theoretical system of vortex beam propagation and provide new solutions for turbulence suppression in practical applications. Table 1 compares several studies on the five turbulence effects discussed in this review.

To characterize the propagation of vortex beams, researchers have adopted a variety of theoretical and numerical methods, each with distinct applicable scopes and inherent constraints. To present the characteristics of these mainstream approaches in a clear and intuitive manner, we provide a comparative summary in Table 2.

Table 1. Examples of studies on five turbulence effects in vortex beam propagation.

Turbulence effect	Beam type	Turbulence model	Research method	Main conclusion
Intensity scintillation	Modified Bessel-Gaussian	Kolmogorov	Extended Huygens-Fresnel, Rytov	Effectively suppresses scintillation;
Beam broadening	Laguerre-Gaussian	Kolmogorov	multi-phase screen method	Larger topological charge leads to higher broadening
Beam wander	Laguerre-Gaussian	Kolmogorov	Rytov approximation, Huygens–Fresnel principle	Wander variance increases with turbulence strength and propagation distance; decreases with increasing topological charge
Angle-of-arrival fluctuation	Vortex beam	Kolmogorov	Optical approximation	Variance increases with turbulence strength and propagation distance
OAM mode crosstalk	Laguerre-Gaussian	Modified von Kármán spectrum	Spiral spectrum analysis, multi-phase screen	OAM crosstalk increases with topological charge

Table 2. Comparison of mainstream research methods for vortex beam propagation.

Method	Core Idea	Applicable Scenario	Limitations
Generalized Huygens-Fresnel Integral	Coherent superposition of spherical secondary waves	Analytical calculation of beam propagation in free space	Applicable to free-space propagation;
Rytov Theory	Optical field = unperturbed field × perturbation term	Weak turbulence	Only applicable to weak turbulence
Born Approximation	Optical field = unperturbed field + perturbation term	Weak turbulence	Only applicable to weak turbulence
phase Screen Method	Stepwise modulation through discrete turbulent phase screens	Numerical simulation of beam propagation	Difficult to accurately simulate the three-dimensional wavefront propagation of vortex beams

3.3 Research Trends in the Propagation Characteristics of Vortex Beams

From the above review of the research background on the propagation of vortex beams in atmospheric turbulence, it can be seen that current domestic and international studies on the turbulent propagation characteristics of vortex beams mainly rely on numerical simulations, and there are still certain theoretical gaps and methodological limitations.

At the methodological level, the phase screen method is a commonly used numerical simulation technique for light propagation in atmospheric turbulence. By applying random phase perturbations to the propagating optical field, it decomposes the overall phase variation caused by atmospheric turbulence into stepwise perturbations of multiple thin phase screens, so as to simulate the beam propagation process in turbulent atmosphere. This method has been widely used in the study of Gaussian beam propagation characteristics, but it has shortcomings when applied to the turbulent propagation simulation of vortex beams. The core feature of vortex beams lies in their helical wavefront, and their special helical phase

structure is prone to irreversible structural distortion after being disturbed by the random phase of phase screens. Meanwhile, the simplified thin-phase-screen approximation cannot accurately reflect the complex interaction between turbulence and the helical phase of vortex beams, eventually leading to deviations between simulation results and real propagation conditions.

At the theoretical modeling level, the vast majority of theoretical derivations directly adopt the classical propagation models of plane waves, spherical waves or Gaussian beams, and describe the turbulent response characteristics of vortex beams through simplifications and approximations. However, owing to the orbital angular momentum they carry, vortex beams possess unique physical characteristics such as helical phase singularities and hollow intensity distributions. Their interaction mechanism with the random fluctuations of the atmospheric refractive index is far more complex than that of traditional Gaussian beams, resulting in insufficient universality and accuracy of theoretical derivations.

In terms of the coverage of turbulence effect research, current studies mostly focus on three types of effects: beam broadening, intensity scintillation, and OAM mode crosstalk. In contrast, only a small number of numerical simulation analyses exist for effects such as beam wander and angle-of-arrival fluctuations, which directly affect the detection accuracy of communication systems, lacking systematic theoretical derivations and experimental verifications. Furthermore, core statistical parameters of atmospheric optical propagation, such as phase scintillation variance, wavefront structure function, and aperture averaging effect, remain almost theoretically unexplored in the field of vortex beams.

4 Introduction to Research Achievements of Xi'an University of Technology

In the field of propagation characteristics of vortex beams in atmospheric turbulence, scholars from various countries have carried out extensive explorations, laying an important foundation for the development of this field. The research group led by Professor Ke Xizheng at Xi'an University of Technology has long focused on vortex optical communication technology, conducted a series of studies on vortex beam generation, detection and propagation characteristics in atmospheric turbulence, and achieved a number of representative research results. The research work in this paper is based on the existing achievements of the team. Aiming at the problem that the field lacks universal analytical models capable of quantifying multiple turbulence effects, it focuses on the core propagation characteristics of vortex beams under weak atmospheric turbulence. This section briefly introduces the relevant research of Professor Ke Xizheng's group at Xi'an University of Technology.

4.1 Intensity Scintillation Variance of Vortex Beams

Owing to the energy distribution characteristics endowed by the helical phase structure, vortex beams present a remarkable advantage in suppressing the intensity scintillation effect during propagation in atmospheric turbulence. At present, most studies on this property mainly adopt numerical simulations and focus on analyzing the variation law of the scintillation index. There is still no quantitative expression for the intensity scintillation variance of vortex beams that covers different turbulence strengths and topological charge conditions, analogous to the expression for Gaussian beams. To address the lack of theoretical models describing intensity scintillation of vortex beams after propagating through atmospheric turbulence, the team derived the log-amplitude fluctuation variance expression for vortex beams under the Kolmogorov turbulence spectrum, based on the Rytov approximation theory and the Huygens–Fresnel principle [14].

$$
\begin{aligned}
\chi^2 = {} & 0.033\,C_n^2 k^4 \int_0^z \frac{dz'}{(z-z')^2} \int_{2\pi/L_0}^{2\pi/l_0} \kappa^{-8/3}\, d\kappa \int_0^{2\pi} \int_0^{\infty} \int_0^{2\pi} \int_0^{\infty} \\
& J_0\left(\kappa\left(\rho'^2+\rho''^2-2\rho'\rho''\cos(\phi'-\phi'')\right)^{1/2}\right) \left\{\left(\frac{\rho'}{\rho}\right)^{|l|}\left(\frac{\sqrt{1+\alpha^2 z^2}}{\sqrt{1+\alpha^2 z'^2}}\right)^{l+1}\right. \\
& \exp\left(\frac{k\alpha\rho^2}{2+2\alpha^2 z^2}-\frac{k\alpha\rho'^2}{2+2\alpha^2 z'^2}\right)\left[\cos\big((l+1)\big(\arctan(\alpha z)-\arctan(\alpha z')\big)\big)\right. \\
& \cos\left(\frac{k\alpha^2\rho'^2 z'}{2+2\alpha^2 z'^2}-\frac{k\alpha^2\rho^2 z}{2+2\alpha^2 z^2}-l\phi'+\frac{k(\rho^2+\rho'^2-2\rho\rho'\cos\phi')}{2(z-z')}\right) \\
& \left.-\sin\big((l+1)\big(\arctan(\alpha z)-\arctan(\alpha z')\big)\big)\right. \\
& \left.\sin\left(\frac{k\alpha^2\rho'^2 z'}{2+2\alpha^2 z'^2}-\frac{k\alpha^2\rho^2 z}{2+2\alpha^2 z^2}-l\phi'+\frac{k(\rho^2+\rho'^2-2\rho\rho'\cos\phi')}{2(z-z')}\right)\right]\Bigg\} \\
& \left\{\left(\frac{\rho''}{\rho}\right)^{|l|}\left(\frac{\sqrt{1+\alpha^2 z^2}}{\sqrt{1+\alpha^2 z'^2}}\right)^{l+1}\right. \\
& \exp\left(\frac{k\alpha\rho^2}{2+2\alpha^2 z^2}-\frac{k\alpha\rho''^2}{2+2\alpha^2 z'^2}\right)\left[\cos\big((l+1)\big(\arctan(\alpha z)-\arctan(\alpha z')\big)\big)\right. \\
& \cos\left(\frac{k\alpha^2\rho''^2 z'}{2+2\alpha^2 z'^2}-\frac{k\alpha^2\rho^2 z}{2+2\alpha^2 z^2}-l\phi''+\frac{k(\rho^2+\rho''^2-2\rho\rho''\cos\phi'')}{2(z-z')}\right) \\
& \left.-\sin\big((l+1)\big(\arctan(\alpha z)-\arctan(\alpha z')\big)\big)\right. \\
& \left.\sin\left(\frac{k\alpha^2\rho''^2 z'}{2+2\alpha^2 z'^2}-\frac{k\alpha^2\rho^2 z}{2+2\alpha^2 z^2}-l\phi''+\frac{k(\rho^2+\rho''^2-2\rho\rho''\cos\phi'')}{2(z-z')}\right)\right]\Bigg\} \\
& \rho'\,d\rho'\,d\phi'\,\rho''\,d\rho''\,d\phi''
\end{aligned}
\tag{42}
$$

where φ denotes the radial angle at the source plane, r is the radial distance at the source plane, ω_0 represents

the initial beam waist, k is the wave number defined as $k = 2\pi/\lambda$, R_0 is the radius of curvature, l is the topological charge, α is a complex parameter expressed as $\alpha = \alpha_r + i\alpha_i = \lambda/\pi a_0^2 + i/R_0$, θ denotes the radial angle at the transmitting end, ρ is the radial distance at the receiving end, and z represents the propagation distance.

4.2 Beam Width of Vortex Beams

Thanks to the unique distribution of orbital angular momentum (OAM), vortex beams exhibit a special response mechanism to the beam broadening effect induced by atmospheric turbulence. However, most existing studies analyze their broadening behavior in turbulent environments via numerical simulations. From the perspective of theoretical modeling, there is still no analytical expression equivalent to that for Gaussian beams which can quantitatively describe the beam width of vortex beams. Our team derived the beam width expression for vortex beams during horizontal propagation in atmospheric turbulence based on the Rytov approximation theory, the Huygens–Fresnel principle, and Andrews' classic wander variance model [15].

$$W_{LT}(z) = \sqrt{\frac{\int_0^\infty \sum_{n=-\infty}^{\infty} \int_0^\infty \int_0^\infty \exp\left[-\left(\frac{1}{\omega_0^2}+\frac{1}{\rho_0^2}+\frac{ik}{2z}\right) r_1^2 - \left(\frac{1}{\omega_0^2}+\frac{1}{\rho_0^2}-\frac{ik}{2z}\right) r_2^2\right] J_n\left(\frac{k\rho}{z} r_1\right) J_n\left(\frac{k\rho}{z} r_2\right) I_{l-n}\left(\frac{2r_1 r_2}{\rho_0^2}\right) (r_1 r_2)^{l+1}\, \mathrm{d}r_1\, \mathrm{d}r_2\, \rho^3 \mathrm{d}\rho}{\int_0^\infty \sum_{n=-\infty}^{\infty} \int_0^\infty \int_0^\infty \exp\left[-\left(\frac{1}{\omega_0^2}+\frac{1}{\rho_0^2}+\frac{ik}{2z}\right) r_1^2 - \left(\frac{1}{\omega_0^2}+\frac{1}{\rho_0^2}-\frac{ik}{2z}\right) r_2^2\right] J_n\left(\frac{k\rho}{z} r_1\right) J_n\left(\frac{k\rho}{z} r_2\right) I_{l-n}\left(\frac{2r_1 r_2}{\rho_0^2}\right) (r_1 r_2)^{l+1}\, \mathrm{d}r_1\, \mathrm{d}r_2\, \rho\, \mathrm{d}\rho}} \tag{43}$$

where ω_0 denotes the initial beam waist width, r_1 and r_2 are the magnitudes of the position vectors of any two points in the source plane, λ represents the transmission wavelength, l is the topological charge of the vortex beam, J_n is the nth-order Bessel function, and I_{l-n} is the modified Bessel function of the first kind of order $(l-n)$, $\rho_0 = (0.545 C_n^2 k^2 z)^{-3/5}$.

4.3 Beam Wander Variance of Vortex Beams

In terms of theoretical modeling, there is still no theoretical expression analogous to that for Gaussian beams which can directly quantify the beam wander variance of vortex beams. To address the challenge of the current lack of a theoretical model describing the spot wander of vortex beams after propagating through atmospheric turbulence, our team derived the expression for the beam wander variance of vortex beams during horizontal propagation in atmospheric turbulence based on Andrews' classic wander variance model [15].

$$\begin{aligned}
\langle \rho_c^2 \rangle = {} & 7.25\, C_n^2 z^2 \int_0^z (1 - z'/z)^2 \\
& \times \left[\left(\frac{\int_0^\infty \sum_{n=-\infty}^{\infty} \int_0^\infty \int_0^\infty \exp\left[-\left(\frac{1}{\omega_0^2}+\frac{1}{\rho_0^2}+\frac{ik}{2z'}\right) r_1^2 - \left(\frac{1}{\omega_0^2}+\frac{1}{\rho_0^2}-\frac{ik}{2z'}\right) r_2^2\right]}{\int_0^\infty \sum_{n=-\infty}^{\infty} \int_0^\infty \int_0^\infty \exp\left[-\left(\frac{1}{\omega_0^2}+\frac{1}{\rho_0^2}+\frac{ik}{2z'}\right) r_1^2 - \left(\frac{1}{\omega_0^2}+\frac{1}{\rho_0^2}-\frac{ik}{2z'}\right) r_2^2\right]} \right. \right. \\
& \left. \cdot \frac{J_n\left(\frac{k\rho}{z'} r_1\right) J_n\left(\frac{k\rho}{z'} r_2\right) I_{l-n}\left(\frac{2r_1 r_2}{\rho_0^2}\right) (r_1 r_2)^{l+1}\, \mathrm{d}r_1\, \mathrm{d}r_2\, \rho^3 \mathrm{d}\rho}{J_n\left(\frac{k\rho}{z'} r_1\right) J_n\left(\frac{k\rho}{z'} r_2\right) I_{l-n}\left(\frac{2r_1 r_2}{\rho_0^2}\right) (r_1 r_2)^{l+1}\, \mathrm{d}r_1\, \mathrm{d}r_2\, \rho\, \mathrm{d}\rho} \right)^{-1/6} \\
& - \left(\frac{\int_0^\infty \sum_{n=-\infty}^{\infty} \int_0^\infty \int_0^\infty \exp\left[-\left(\frac{1}{\omega_0^2}+\frac{1}{\rho_0^2}+\frac{ik}{2z'}\right) r_1^2\right]}{\int_0^\infty \sum_{n=-\infty}^{\infty} \int_0^\infty \int_0^\infty \exp\left[-\left(\frac{1}{\omega_0^2}+\frac{1}{\rho_0^2}+\frac{ik}{2z'}\right) r_1^2\right]} \right. \\
& \left. \left. \cdot \frac{\exp\left[-\left(\frac{1}{\omega_0^2}+\frac{1}{\rho_0^2}-\frac{ik}{2z'}\right) r_2^2\right] J_n\left(\frac{k\rho}{z'} r_1\right) J_n\left(\frac{k\rho}{z'} r_2\right) I_{l-n}\left(\frac{2r_1 r_2}{\rho_0^2}\right) (r_1 r_2)^{l+1}\, \mathrm{d}r_1\, \mathrm{d}r_2\, \rho^3 \mathrm{d}\rho}{\exp\left[-\left(\frac{1}{\omega_0^2}+\frac{1}{\rho_0^2}-\frac{ik}{2z'}\right) r_2^2\right] J_n\left(\frac{k\rho}{z'} r_1\right) J_n\left(\frac{k\rho}{z'} r_2\right) I_{l-n}\left(\frac{2r_1 r_2}{\rho_0^2}\right) (r_1 r_2)^{l+1}\, \mathrm{d}r_1\, \mathrm{d}r_2\, \rho\, \mathrm{d}\rho} + \frac{1}{K_0^2} \right)^{-1/6} \right] \mathrm{d}z'
\end{aligned} \tag{44}$$

where ω_0 is the initial beam waist radius; l is the topological charge; k is the wavenumber; λ is the wavelength; $\kappa_0 = 1/L_0$, L_0 is the outer scale size of turbulence; J_n is the nth-order Bessel function, and I_{l-n} is the modified Bessel function of the first kind of order $(l-n)$. $\rho_0 = (0.545 C_n^2 k^2 z)^{-3/5}$.

4.4 Angle-of-Arrival Fluctuation Variance of Vortex Beams

Compared with other turbulence effects, there are relatively few studies on the angle-of-arrival fluctuation effect of vortex beams. Currently, there is still a lack of a theoretical model describing the angle-of-arrival fluctuations of vortex beams after propagation through atmospheric turbulence. Based on the optical approximation, our team derived the expression for the angle-of-arrival fluctuation variance of vortex beams after passing through the turbulent

layer [89]:

$$\sigma_\alpha^2 = 2.94\,C_n^2 \int_0^L \Bigg[\frac{\int_0^\infty \sum_{n=-\infty}^{\infty} \int_0^\infty \int_0^\infty \exp\left[-\left(\frac{1}{\omega_0^2}+\frac{1}{\rho_0^2}\right)(r_1^2+r_2^2)\right] \exp\left[-\frac{ik}{2z}(r_1^2-r_2^2)\right]}{\int_0^\infty \sum_{n=-\infty}^{\infty} \int_0^\infty \int_0^\infty \exp\left[-\left(\frac{1}{\omega_0^2}+\frac{1}{\rho_0^2}\right)(r_1^2+r_2^2)\right] \exp\left[-\frac{ik}{2z}(r_1^2-r_2^2)\right]} \cdot \frac{J_n\left(\frac{k\rho r_1}{z}\right) J_n\left(\frac{k\rho r_2}{z}\right) I_{n+l}\left(\frac{2r_1 r_2}{\rho_0^2}\right) r_1 r_2\,\mathrm{d}r_1\,\mathrm{d}r_2\,\rho^3\mathrm{d}\rho}{J_n\left(\frac{k\rho r_1}{z}\right) J_n\left(\frac{k\rho r_2}{z}\right) I_{n+l}\left(\frac{2r_1 r_2}{\rho_0^2}\right) r_1 r_2\,\mathrm{d}r_1\,\mathrm{d}r_2\,\rho\,\mathrm{d}\rho} \Bigg]^{-\frac{1}{6}} \mathrm{d}z \tag{45}$$

where r_1 and r_2 are the magnitudes of the position vectors of any two points in the source plane; J_n is the nth-order Bessel function, and I_{l-n} is the modified Bessel function of the first kind of order $(l-n)$.

Numerical simulations of Equations (42) to (45) show that, as the propagation distance increases, the beam width, intensity scintillation variance, wander variance, and angle-of-arrival fluctuation variance of vortex beams with different topological charges all exhibit a significant increasing trend.

Increasing the topological charge broadens the beam width of the vortex beam while effectively reducing the intensity scintillation variance, beam wander variance, and angle-of-arrival fluctuation variance. Enhanced turbulence strength causes all four propagation characteristic indicators to rise simultaneously, with an especially pronounced impact on the beam wander variance. When the wavelength and initial beam waist are increased, the beam width of the vortex beam increases accordingly, while the beam wander variance and angle-of-arrival fluctuation variance show a decreasing trend. Among these, increasing the initial beam waist is an effective method to suppress beam wander caused by atmospheric turbulence.

5 Conclusions and Future Prospects

The research on the propagation characteristics of vortex beams under atmospheric turbulence is the core foundation for advancing vortex optical communication technology from theoretical research to engineering applications, and it also represents an important research direction in the field of free-space optical communications. Throughout the development of this field, the vast majority of related studies have adopted the multi-phase screen method to simulate atmospheric turbulence environments and analyze the evolution laws of effects such as intensity scintillation, beam broadening, and orbital angular momentum (OAM) mode crosstalk of different types of vortex beams in turbulence. However, the mainstream multi-phase screen methods are mostly designed for plane waves, which limits the accuracy and reliability of simulation results for vortex wavefront propagation. At the same time, the field still lacks universally applicable analytical theoretical models that can accurately quantify various turbulence effects on vortex beams, and a theoretical framework for describing propagation characteristics equivalent to that for conventional Gaussian beams has not yet been established.

To address this issue, Professor Ke Xizheng's research team at Xi'an University of Technology has conducted systematic studies on the propagation characteristics of vortex beams under weak atmospheric turbulence. Based on classical theories such as the Rytov perturbation method and the generalized Huygens–Fresnel principle, the team has successively derived analytical forms for the intensity scintillation variance, beam width expression, beam wander variance, and angle-of-arrival fluctuation variance of vortex beams, providing important theoretical support for the analysis of turbulence effects on vortex beams. Despite these advances, most of the existing analytical expressions suffer from high computational complexity due to nested multiple integrals, limiting their engineering practicability. Thus, simplified and concise analytical results need to be obtained through reasonable model simplification and mathematical derivation. Meanwhile, current theoretical studies are mostly confined to the weak turbulence regime, and the research scope has not been systematically extended to strong turbulence environments. The propagation and evolution laws of vortex beams under strong turbulence remain to be explored, and a theoretical system for vortex beam propagation covering the full range of turbulence intensities still needs to be improved.

Although extensive research has been carried out in this field, existing work mostly focuses on macroscopic turbulence effects such as intensity scintillation, beam broadening, and beam wander. There is still a lack of systematic research tailored to vortex beams for important statistical quantities that determine the core propagation performance of vortex beams, including phase fluctuation variance, phase structure function, and aperture averaging factor.

Phase fluctuation variance is an important parameter quantifying the degree of random distortion of the

helical wavefront under turbulence perturbations. It reflects the propagation stability of topological charges and the evolution of phase singularities of vortex beams, and is the basis for analyzing the OAM mode propagation characteristics of vortex beams. Current studies on this parameter mostly directly adopt classical calculation models for plane waves, without fully accounting for the helical phase structure and OAM mode characteristics of vortex beams. Future work can build analytical models of phase fluctuation variance tailored to the intrinsic helical phase characteristics of vortex beams in regimes from weak to moderate-strong turbulence, based on the Rytov perturbation theory and the extended Rytov method. These models will accurately quantify the distortion characteristics of the helical wavefront under different topological charges, propagation distances, and turbulence intensities, and clarify the intrinsic correlation between turbulence-induced phase distortion and OAM mode crosstalk.

As an indicator characterizing the spatial correlation of wavefront phase at two points caused by turbulence, the phase structure function is the foundation for constructing analytical theories of vortex beam propagation and quantifying the spatial distribution characteristics of phase distortion. It also serves as an important theoretical basis for designing turbulence effect compensation schemes. Existing studies have not yet established a general calculation model for the phase structure function adapted to the phase characteristics of vortex beams. Future research can derive general analytical expressions for the phase structure function covering the full range of turbulence intensities, based on the Kolmogorov turbulence theory framework, combined with the modified von Karman turbulence spectrum and Tatarskii spectrum, and introducing the topological charge and OAM mode characteristics of vortex beams. This will clarify the regulation laws of key beam parameters on the spatial correlation of wavefront phase, and provide support for the improvement of the analytical theory of vortex beam propagation in turbulence.

The aperture averaging factor is a key parameter measuring the suppression effect of the receiving aperture on turbulence-induced intensity fluctuations. It is directly related to the received signal-to-noise ratio (SNR) and link reliability of vortex-based free-space optical communication systems, and is a core parameter for the design of engineering receiving systems. Existing studies on the aperture averaging factor mostly focus on Gaussian beams and plane waves. Future work can combine the annular intensity distribution characteristics of vortex beams with classical aperture reception theory to derive quantitative calculation models of the aperture averaging factor under different turbulence intensities, receiving aperture sizes, and topological charges, and clarify the suppression limits and performance optimization directions of the aperture averaging effect on the intensity scintillation of vortex beams.

In general, research on the above and many other unmentioned statistical quantities, as well as the improvement of the analytical theoretical system covering the full turbulence range, constitute the important theoretical foundation for advancing the engineering application of vortex optical communications, and are also important research directions to be addressed in this field in the future.

Data Availability Statement

Not applicable.

Funding

This work was supported in part by the Key Industrial Innovation Chain Project of Shaanxi Province under Grant 2017ZDCXL-GY-06-01, and in part by the National Natural Science Foundation of China (NSFC) under Grant 61377080.

Conflicts of Interest

Xizheng Ke served as an Editor-in-Chief of the *Optical Wireless Communication* at the time of manuscript submission. To ensure the integrity of the peer-review process, Xizheng Ke was not involved in the editorial handling, peer review, or decision-making process for this manuscript, which was handled independently by another editor. The remaining authors declare no conflicts of interest.

AI Use Statement

The authors declare that no generative AI was used in the preparation of this manuscript.

Ethical Approval and Consent to Participate

Not applicable.

References

[1] Khalighi, M. A., & Uysal, M. (2014). Survey on free space optical communication: A communication

theory perspective. *IEEE communications surveys & tutorials, 16*(4), 2231-2258. [CrossRef]

[2] Tan, Y., & Guo, J. Z. (2005, September). Study of channel model of free-space laser communications system. In *Free-Space Laser Communications V* (Vol. 5892, pp. 587-594). SPIE. [CrossRef]

[3] Abdourahamane, A. (2016). Advantages of optical orthogonal frequency division multiplexing in communications systems. *EUREKA: Physics and Engineering*, (2), 27-33. [CrossRef]

[4] Zhao, Y., Yu, G., & Xu, H. (2019). 6G mobile communication network: vision, challenges, and key technologies. *Scientia Sinica Informationis, 49*(8), 963-987. [CrossRef]

[5] Bai, Y., Lv, H., Fu, X., & Yang, Y. (2022). Vortex beam: generation and detection of orbital angular momentum. *Chinese Optics Letters, 20*(1), 012601. https://opg.optica.org/col/abstract.cfm?uri=col-20-1-012601

[6] Pope, S. B. (2001). Turbulent flows. *Measurement Science and Technology, 12*(11), 2020-2021. [CrossRef]

[7] Guo, Q., Song, P., Zhang, Z. Q., ZHOU, A., & QU, P. (2020). Research on the key technology of turbulence suppression for atmos-pheric optical laser communication based on OFDM. *Opto-Electronic Engineering, 47*(3), 190619. [CrossRef]

[8] Zhao, W., & Chen, C. (2024, April). Simulation Method for the Impact of Atmospheric Wind Speed on Optical Signals in Satellite–Ground Laser Communication Links. In *Photonics* (Vol. 11, No. 5, p. 417). MDPI. [CrossRef]

[9] Rao, R. (2005, May). Optical properties of atmospheric turbulence and their effects on light propagation. In *Optical Technologies for Atmospheric, Ocean, and Environmental Studies* (Vol. 5832, pp. 1-11). SPIE. [CrossRef]

[10] Fante, R. L. (1975). Electromagnetic beam propagation in turbulent media. *Proceedings of the IEEE, 63*(12), 1669-1692. [CrossRef]

[11] Tatarski, V. I., Silverman, R. A., & Chako, N. (1961). Wave Propagation in a Turbulent Medium. *Physics Today, 14*(12), 46-51. [CrossRef]

[12] Ke, X. (2025). *Partially Coherent Optical Transmission Theory in Optical Wireless Communication*. Springer Nature Singapore. [CrossRef]

[13] Ishimaru, A. (1978). *Wave propagation and scattering in random media* (Vol. 2, pp. 148-166). New York: Academic press. [CrossRef]

[14] Ke, X. Z., & Li, X. W. (2025). Light intensity scintillation of a vortex beam after propagation in weak turbulence. *Optics Communications*, *592*, 132215. [CrossRef]

[15] Ke, X. Z., & Li, X. W. (2025). Vortex beam broadening and wander in atmospheric turbulence. *Journal of Applied Physics*, *138*(14), 143102. [CrossRef]

[16] Andrews, L. C., & Phillips, R. L. (2005). *Laser beam propagation through random media* (2nd ed.). SPIE Press. [CrossRef]

[17] Phillips, R. L., & Andrews, L. C. (1983). Spot size and divergence for Laguerre Gaussian beams of any order. *Applied optics, 22*(5), 643-644. [CrossRef]

[18] Xizheng, K., Chuan, N., & Jiao, W. (2018). Crosstalk analysis of orbital angular momentum-multiplexed state under atmospheric turbulence. *Infrared and laser engineering, 47*(11), 1122002-1122002. [CrossRef]

[19] Nye, J. F., & Berry, M. V. (1974). Dislocations in Wave Trains. *Proceedings of the Royal Society of London Series A, 336*(1605), 165-190. [CrossRef]

[20] Dong, M., Zhao, C., Cai, Y., & Yang, Y. (2021). Partially coherent vortex beams: Fundamentals and applications. *Science China Physics, Mechanics & Astronomy, 64*(2), 224201. [CrossRef]

[21] Boivin, A., Dow, J., & Wolf, E. (1967). Energy flow in the neighborhood of the focus of a coherent beam. *Journal of the Optical Society of America, 57*(10), 1171-1175. [CrossRef]

[22] Coullet, P., Gil, L., & Rocca, F. (1989). Optical vortices. *Optics Communications, 73*(5), 403-408. [CrossRef]

[23] Allen, L., Beijersbergen, M. W., Spreeuw, R. J. C., & Woerdman, J. P. (1992). Orbital angular momentum of light and the transformation of Laguerre-Gaussian laser modes. *Physical review A, 45*(11), 8185. [CrossRef]

[24] Barnett, S. M., & Allen, L. (1994). Orbital angular momentum and nonparaxial light beams. *Optics communications, 110*(5-6), 670-678. [CrossRef]

[25] Beijersbergen, M. W., Coerwinkel, R. P. C., Kristensen, M., & Woerdman, J. P. (1994). Helical-wavefront laser beams produced with a spiral phaseplate. *Optics communications, 112*(5-6), 321-327. [CrossRef]

[26] He, H., Friese, M. E. J., Heckenberg, N. R., & Rubinsztein-Dunlop, H. (1995). Direct observation of transfer of angular momentum to absorptive particles from a laser beam with a phase singularity. *Physical review letters, 75*(5), 826. [CrossRef]

[27] Durnin, J. J. J. A. (1987). Exact solutions for nondiffracting beams. I. The scalar theory. *Journal of the Optical Society of America A, 4*(4), 651-654. [CrossRef]

[28] Volke-Sepúlveda, K., Garcés-Chávez, V., Chávez-Cerda, S., Arlt, J., & Dholakia, K. (2002). Orbital angular momentum of a high-order Bessel light beam. *Journal of Optics B: Quantum and Semiclassical Optics, 4*(2), S82-S89. [CrossRef]

[29] Khonina, S. N., Kazanskiy, N. L., Khorin, P. A., & Butt, M. A. (2021). Modern types of axicons: New functions and applications. *Sensors, 21*(19), 6690. [CrossRef]

[30] Xie, Q., & Zhao, D. (2008). Optical vortices generated by multi-level achromatic spiral phase plates for broadband beams. *Optics communications, 281*(1), 7-11. [CrossRef]

[31] Yu, N., Genevet, P., Kats, M. A., Aieta, F., Tetienne, J. P., Capasso, F., & Gaburro, Z. (2011). Light

propagation with phase discontinuities: generalized laws of reflection and refraction. *science, 334*(6054), 333-337. [CrossRef]

[32] Forbes, A., Dudley, A., & McLaren, M. (2016). Creation and detection of optical modes with spatial light modulators. *Advances in Optics and Photonics*, *8*(2), 200–227. [CrossRef]

[33] Wang, T., Wang, F., Shi, F., Pang, F., Huang, S., Wang, T., & Zeng, X. (2017). Generation of femtosecond optical vortex beams in all-fiber mode-locked fiber laser using mode selective coupler. *Journal of Lightwave Technology, 35*(11), 2161-2166. [CrossRef]

[34] Du, J., & Wang, J. (2017). Chip-scale optical vortex lattice generator on a silicon platform. *Optics Letters*, *42*(23), 5054–5057. [CrossRef]

[35] Zelenchuk, D., & Fusco, V. (2013). Split-ring FSS spiral phase plate. *IEEE Antennas and Wireless Propagation Letters, 12*, 284-287. [CrossRef]

[36] Xu, X., Qian, X. M., Luo, C. K., Chen, X. W., Cui, C. L., & Zhu, W. Y. (2023). Experimental study of the transport characteristics of fractional-order vortex beams in a turbulent atmosphere simulator. *AIP Advances, 13*(9). [CrossRef]

[37] Zhao, W., Yu, S., & Kou, N. (2025). Stable divergence angle control of OAM vortex beams with different modes. *Physics Letters A, 541*, 130428. [CrossRef]

[38] Liu, X., Li, Y., Yao, G., Li, C., Fang, B., Tang, Y., ... & Jing, X. (2024). Perfect vortex beams generation based on reflective geometric phase metasurfaces. *Chinese Journal of Physics, 91*, 828-837. [CrossRef]

[39] Wang, H., Fu, S., & Gao, C. (2021). Tailoring a complex perfect optical vortex array with multiple selective degrees of freedom. *Optics Express, 29*(7), 10811-10824. [CrossRef]

[40] Gibson, G., Courtial, J., Padgett, M. J., Vasnetsov, M., Pas' ko, V., Barnett, S. M., & Franke-Arnold, S. (2004). Free-space information transfer using light beams carrying orbital angular momentum. *Optics express, 12*(22), 5448-5456. [CrossRef]

[41] Elder, H. F., & Sprangle, P. (2022). Mode power spectrum for Laguerre–Gauss beams in Kolmogorov turbulence. *Optics Letters, 47*(14), 3447-3450. [CrossRef]

[42] Charnotskii, M. (2015). Extended Huygens–Fresnel principle and optical waves propagation in turbulence: discussion. *Journal of the Optical Society of America A, 32*(7), 1357-1365. [CrossRef]

[43] Mei, Z., Shchepakina, E., & Korotkova, O. (2013). Propagation of cosine-Gaussian-correlated Schell-model beams in atmospheric turbulence. *Optics express, 21*(15), 17512-17519. [CrossRef]

[44] Eyyuboğlu, H. T., Baykal, Y., Sermutlu, E., Korotkova, O., & Cai, Y. (2009). Scintillation index of modified Bessel–Gaussian beams propagating in turbulent media. *Journal of the Optical Society of America A, 26*(2), 387-394. [CrossRef]

[45] Berman, G. P., Gorshkov, V. N., & Torous, S. V. (2011, February). Scintillation reduction for combined Gaussian-vortex beam propagating through turbulent atmosphere. In *Atmospheric and Oceanic Propagation of Electromagnetic Waves V* (Vol. 7924, pp. 94-106). SPIE. [CrossRef]

[46] Xu, Y., Li, Y., & Zhao, X. (2015). Intensity and effective beam width of partially coherent Laguerre–Gaussian beams through a turbulent atmosphere. *Journal of the Optical Society of America A, 32*(9), 1623-1630. [CrossRef]

[47] Li, J., Zhang, H., & Lü, B. (2010). Partially coherent vortex beams propagating through slant atmospheric turbulence and coherence vortex evolution. *Optics & Laser Technology, 42*(2), 428-433. [CrossRef]

[48] Liu, D., Wang, Y., & Yin, H. (2016). Propagation properties of partially coherent four-petal Gaussian vortex beams in turbulent atmosphere. *Optics & Laser Technology, 78*, 95-100. [CrossRef]

[49] Hricha, Z., Lazrek, M., Yaalou, M., & Belafhal, A. (2021). Effects of turbulent atmosphere on the propagation properties of vortex Hermite-cosine-hyperbolic-Gaussian beams. *Optical and Quantum Electronics, 53*(11), 624. [CrossRef]

[50] Chen, D., Li, J., Zhou, Y., & Dong, K. (2025). Propagation characteristics of off-axis Laguerre–Gaussian vortex beam in an oceanic turbulent stratified oblique channel. *Applied Optics, 64*(28), 8425-8434. [CrossRef]

[51] Odžak, S. (2025). Propagation of standard and elegant Laguerre–Gaussian vortex beams through a gradient-index medium. Optical and Quantum Electronics, 57(5), 300. [CrossRef]

[52] Zhong, Y., Cui, Z., Shi, J., & Qu, J. (2011). Propagation properties of partially coherent Laguerre–Gaussian beams in turbulent atmosphere. *Optics & Laser Technology, 43*(4), 741-747. [CrossRef]

[53] Lukin, V. P., Konyaev, P. A., & Sennikov, V. A. (2012). Beam spreading of vortex beams propagating in turbulent atmosphere. *Applied optics, 51*(10), C84-C87. [CrossRef]

[54] Zhou, G. (2006). Analytical vectorial structure of Laguerre–Gaussian beam in the far field. *Optics letters, 31*(17), 2616-2618. [CrossRef]

[55] Luo, C., & Han, X. E. (2020). Evolution and Beam spreading of Arbitrary order vortex beam propagating in atmospheric turbulence. *Optics Communications, 460*, 124888. [CrossRef]

[56] Lazrek, M., Hricha, Z., & Belafhal, A. (2022). Propagation properties of vortex cosine-hyperbolic-Gaussian beams through oceanic turbulence. *Optical and Quantum Electronics, 54*(3), 172. [CrossRef]

[57] Pan, Y., Zhao, M., Zhang, M., Dou, J., Zhao, J.,

Li, B., & Hu, Y. (2023). Propagation properties of rotationally-symmetric power-exponent-phase vortex beam through oceanic turbulence. *Optics & Laser Technology, 159*, 109024. [CrossRef]

[58] Flossmann, F., Schwarz, U. T., & Maier, M. (2005). Propagation dynamics of optical vortices in Laguerre–Gaussian beams. *Optics Communications, 250*(4-6), 218-230. [CrossRef]

[59] Padgett, M. (2024). Orbital angular momentum of single photons: revealing quantum fundamentals. *Philosophical transactions. Series A, Mathematical, physical, and engineering sciences, 382*(2287), 20230327. [CrossRef]

[60] Zeng, J., Liu, X., Zhao, C., Wang, F., Gbur, G., & Cai, Y. (2019). Spiral spectrum of a Laguerre-Gaussian beam propagating in anisotropic non-Kolmogorov turbulent atmosphere along horizontal path. *Optics Express, 27*(18), 25342-25356. [CrossRef]

[61] Yao, M., Toselli, I., & Korotkova, O. (2014). Propagation of electromagnetic stochastic beams in anisotropic turbulence. *Optics express, 22*(26), 31608-31619. [CrossRef]

[62] Wei, H., Du, Q., Shi, C., Xue, X., & Cai, D. (2023). Crosstalk characteristics of orbital angular momentum of focused perfect vortex beam in atmospheric turbulence. *Laser Physics, 33*(11), 115402. [CrossRef]

[63] Jiang, Y., Wang, S., Zhang, J., Ou, J., & Tang, H. (2013). Spiral spectrum of Laguerre–Gaussian beam propagation in non-Kolmogorov turbulence. *Optics communications, 303*, 38-41. [CrossRef]

[64] Cerjan, A., & Cerjan, C. (2011). Orbital angular momentum of Laguerre–Gaussian beams beyond the paraxial approximation. *Journal of the Optical Society of America A, 28*(11), 2253-2260. [CrossRef]

[65] Lv, H., Ren, C., & Liu, X. (2020). Orbital angular momentum spectrum of partially coherent vortex beams in slant atmospheric turbulence. *Infrared Physics & Technology, 105*, 103181. [CrossRef]

[66] Cheng, M., Guo, L., Li, J., & Huang, Q. (2016). Propagation properties of an optical vortex carried by a Bessel–Gaussian beam in anisotropic turbulence. *Journal of the Optical Society of America A, 33*(8), 1442-1450. [CrossRef]

[67] Wang, H., Yang, Z., Liu, L., Chen, Y., Wang, F., & Cai, Y. (2023). Orbital angular momentum spectra of twisted Laguerre-Gaussian Schell-model beams propagating in weak-to-strong Kolmogorov atmospheric turbulence. *Optics Express, 31*(2), 916-928. [CrossRef]

[68] Guo, Y., Bai, L., Wang, Y., Gao, P., & Guo, L. (2021). Reducing orbital angular momentum modes crosstalk of Bessel Gaussian beams in anisotropic atmospheric turbulence with Localized Wave. *Optik, 248*, 167995. [CrossRef]

[69] Murakami, Y., Kishikawa, H., & Goto, N. (2021, July). Comparative Studies of Atmospheric Turbulence Effects on Orbital Angular Momentum Beams. In *Optoelectronics and Communications Conference* (pp. JS3E-6). Optica Publishing Group. [CrossRef]

[70] Knepp, D. L. (1983). Multiple phase-screen calculation of the temporal behavior of stochastic waves. *Proceedings of the IEEE, 71*(6), 722-737. [CrossRef]

[71] Liu, X., & Pu, J. (2011). Investigation on the scintillation reduction of elliptical vortex beams propagating in atmospheric turbulence. *Optics express, 19*(27), 26444-26450. [CrossRef]

[72] Rodenburg, B., Mirhosseini, M., Malik, M., Magaña-Loaiza, O. S., Yanakas, M., Maher, L., ... & Boyd, R. W. (2014). Simulating thick atmospheric turbulence in the lab with application to orbital angular momentum communication. *New Journal of Physics, 16*(3), 033020. [CrossRef]

[73] Banakh, V. A., & Falits, A. V. (2014). Turbulent broadening of Laguerre-Gaussian beam in the atmosphere. *Optics and Spectroscopy, 117*(6), 942-948. [CrossRef]

[74] Porfirev, A. P., Kirilenko, M. S., Khonina, S. N., Skidanov, R. V., & Soifer, V. A. (2017). Study of propagation of vortex beams in aerosol optical medium. *Applied Optics, 56*(11), E8-E15. [CrossRef]

[75] Fu, S., & Gao, C. (2016). Influences of atmospheric turbulence effects on the orbital angular momentum spectra of vortex beams. *Photonics Research, 4*(5), B1-B4. [CrossRef]

[76] Filimonov, G. A., Aksenov, V. P., Kolosov, V. V., & Pogutsa, C. E. (2016, November). Fluctuations of the orbital angular momentum of vortex laser beam in turbulent atmosphere: dependence on turbulence strength and beam parameters. In *22nd International Symposium on Atmospheric and Ocean Optics: Atmospheric Physics* (Vol. 10035, pp. 525-530). SPIE. [CrossRef]

[77] Eyyuboğlu, H. T. (2016). Scintillation behaviour of vortex beams in strong turbulence region. *Journal of Modern Optics, 63*(21), 2374-2381. [CrossRef]

[78] Wang, L. G., & Zheng, W. W. (2009). The effect of atmospheric turbulence on the propagation properties of optical vortices formed by using coherent laser beam arrays. *Journal of Optics A: Pure and Applied Optics, 11*(6), 065703. [CrossRef]

[79] Li, J., Liang, H., Wu, G., Peng, P., Wang, F., & Cai, Y. (2025). Generation of vector vortex pin-like beams and their propagation in turbulent atmosphere. *APL Photonics, 10*(1). [CrossRef]

[80] Su, Q. Q. (2025). Propagation of polarized double-elliptical vortex beams in atmospheric turbulence. *Applied Optics, 64*(23), 6557-6563. [CrossRef]

[81] Xu, X., Luo, C., Qian, X., & Zhu, W. (2024, August). Investigation of the propagation characteristics of double-ring perfect vortex beams in atmospheric turbulence. In *Photonics* (Vol. 11, No. 8, p. 768). MDPI.

[CrossRef]

[82] Zhang, Z., Li, G., Liu, Y., Wang, H., Hoenders, B. J., Liang, C., ... & Zeng, J. (2024). Robust measurement of orbital angular momentum of a partially coherent vortex beam under amplitude and phase perturbations. *Opto-Electronic Science, 3*(1), 240001-1. [CrossRef]

[83] Tang, S., Yan, J., Yong, K., & Zhang, R. (2019). Propagation characteristics of vortex beams in anisotropic atmospheric turbulence. *Journal of the Optical Society of America B, 37*(1), 133-137. [CrossRef]

[84] Hu, P., Zhu, L., Zhu, J., Ren, J., Chen, S., Ma, J., ... & Liu, B. (2024). Physics-driven untrained neural network for vortex beam compensation in adaptive optics aided underwater wireless optical communications. *Optics Express, 32*(27), 47936-47958. [CrossRef]

[85] Al-Ahsab, H. T., Cheng, Q., Cheng, M., Guo, L., Cao, Y., & Wang, S. (2023). Propagation behavior of orbital angular momentum in vector anomalous vortex beams under maritime atmospheric turbulence. *Frontiers in Physics, 11*, 1238101. [CrossRef]

[86] Singh, S., Mishra, S. K., & Mishra, A. K. (2024). Evolutions of a ring Airy vortex beam and a ring Pearcey vortex beam in turbulent atmosphere and a comparative analysis of their channel efficiencies and OAM spectra. *Applied Optics, 63*(26), 6845-6853. [CrossRef]

[87] Xu, D., Lu, Z., Wang, Y., Liu, H., Duan, S., Lin, W., ... & Liu, B. (2025). Propagation dynamics of autofocusing Mathieu vortex beams through atmospheric turbulence. *Optics Communications, 579*, 131569. [CrossRef]

[88] Gökçe, M. C., Baykal, Y., Gerçekcioğlu, H., & Ata, Y. (2024). Intensity and degree of coherence of vortex beams in atmospheric turbulence. *IEEE Journal of Quantum Electronics, 60*(6), 1-8. [CrossRef]

[89] Ke, X., & Wang, J. (2023). *Generation, transmission, detection, and application of vortex beams* (Vol. 447). Singapore: Springer. [CrossRef]

Xiwen Li is currently a Master's student at the School of Automation and Information Engineering, Xi'an University of Technology. His research interests focus on wireless optical communications. (Email: 1158436960@qq.com)

Jingyuan Liang holds a master's degree and works as an Assistant Engineer. Her primary research is dedicated to modulation and demodulation technologies for wireless optical communication systems. (Email: ljy@xaut.edu.cn)

Xizheng Ke, born in 1962, holds a PhD in Science and works as a Level II Professor at Xi'an University of Technology. He is a Foreign Member of the Russian Academy of Natural Sciences, Distinguished Teaching Master of Shaanxi Province, and Fellow of the Chinese Institute of Electronics. His main research interests lie in the theory and technology of wireless optical communications. (Email: xzke@263.net)